

Review

Open Access



Rigid-flexible coupling poly (phenylene sulfide) fiber membrane: a highly stable chemical and thermal material for energy and environmental applications

Qixuan Zhu, Tao Zhang, Xiaoqing Zhu, Jia Zhang, Minghui Shan, Zexu Hu, Guiyin Xu*, Meifang Zhu

State Key Laboratory for Modification of Chemical Fibers and Polymer Materials, College of Materials Science and Engineering, Donghua University, Shanghai 201620, China.

*Correspondence to: Prof. Guiyin Xu, State Key Laboratory for Modification of Chemical Fibers and Polymer Materials, College of Materials Science and Engineering, Donghua University, 2999 Renmin North Road, Shanghai 201620, China. E-mail: xuguiyin@dhu.edu.cn

How to cite this article: Zhu Q, Zhang T, Zhu X, Zhang J, Shan M, Hu Z, Xu G, Zhu M. Rigid-flexible coupling poly (phenylene sulfide) fiber membrane: a highly stable chemical and thermal material for energy and environmental applications. *Energy Mater* 2024;4:400016. <https://dx.doi.org/10.20517/energymater.2023.85>

Received: 27 Oct 2023 **First Decision:** 21 Dec 2023 **Revised:** 26 Dec 2023 **Accepted:** 1 Feb 2024 **Published:** 1 Mar 2024

Academic Editor: Yuping Wu **Copy Editor:** Fangling Lan **Production Editor:** Fangling Lan

Abstract

The poly (phenylene sulfide) (PPS) fiber membrane is composed of interwoven fibers, with a three-dimensional porous structure. The three-dimensional porous structure makes PPS fiber membranes have high porosity and large specific surface area, which stands out in the field of membrane separation. A PPS fiber is a high-performance fiber with excellent chemical and thermal stability. These characteristics allow PPS fiber membranes to be used in harsh membrane separation environments such as strong acids, alkalis, and high temperatures. However, the corrosion resistance and high-temperature stability of PPS fibers also make the preparation of PPS fibers and their membranes challenging. In this paper, the preparation method is summarized, including two direct methods to make a PPS fiber membrane: melt-blown spinning and melt electrostatic spinning, and two indirect methods: wet papermaking and weaving. Additionally, the applications of PPS fiber membranes are summarized in detail in energy and environmental fields, such as lithium-ion batteries, alkaline water electrolysis, air filtrations, chemical catalyst substrates, and oil-water separations. This review provides an insightful understanding of PPS fiber membrane preparation methods and the interconnections between these preparation methods and specific applications, thus laying a solid foundation for further advancing the range of PPS fiber membrane applications.

Keywords: PPS fiber membrane, preparation method, energy and environmental applications



© The Author(s) 2024. **Open Access** This article is licensed under a Creative Commons Attribution 4.0 International License (<https://creativecommons.org/licenses/by/4.0/>), which permits unrestricted use, sharing, adaptation, distribution and reproduction in any medium or format, for any purpose, even commercially, as long as you give appropriate credit to the original author(s) and the source, provide a link to the Creative Commons license, and indicate if changes were made.



INTRODUCTION

Separation technology is an important branch of modern industry. However, traditional separation techniques, including evaporation^[1], centrifugation^[2], extraction^[3], ion exchange^[4], *etc.*, often suffer from process complexity, limited selectivity, and high cost. Since the 1960s, a new separation technology known as membrane separation technology has emerged rapidly^[5]. This technology not only offers separation, concentration, and purification capabilities but also boasts the advantages of simplicity, high efficiency, energy conservation, and environmental friendliness^[6]. Currently, membrane separation technology finds widespread application in various fields such as food^[7], medicine^[8], chemical industry^[9], energy^[10], environmental protection^[11], and water treatment^[12]. Despite the many advantages of membrane separation technology, there is large demand on the separation membrane materials in the harsh environment of high temperatures and strong corrosion. Based on the membrane material, membranes can be classified into ceramic and polymer types. Ceramic membranes exhibit exceptional thermal stability and corrosion resistance, but they are challenging to process and lack toughness, limiting their use primarily to the food and pharmaceutical sectors^[13]. In contrast, polymer membranes, with their easy process, good toughness, and cost-effectiveness, have become one of the most commonly employed membrane materials in the field of membrane separation^[14]. However, conventional polymer materials [polyethylene (PE), polypropylene (PP), *etc.*] do not exhibit both excellent thermal and chemical stability concurrently. For example, PE has excellent chemical stability below 80 °C, but it has a high service temperature of 140 °C^[15]. Therefore, there is a need for a membrane material that can remain stable and efficient over a long period of time in high-temperature and highly corrosive membrane separation scenarios.

Poly (phenylene sulfide) (PPS) is a thermoplastic polymer material with excellent high-temperature stability, corrosion resistance and flame-retardant properties. The glass transition temperature, melting temperature, and decomposition temperature of PPS are 85, 285, and 490 °C, respectively^[16]. The molecular chain of PPS consists of benzene rings alternating with sulfur atoms. The benzene ring structure imparts heightened rigidity to PPS, and the sulfur atom contributes to the flexibility performance^[17]. These unique structures result in PPS fibers having excellent high thermal stability, corrosion resistance, and flame retardancy. These excellent properties allow PPS fibers and their fiber membranes not only to have a long lifetime at temperatures as high as 200 °C but also to resist most of the strong acids and alkalis. In addition, the three-dimensional interlaced fiber membrane structure endows the PPS fiber membrane with high porosity and large specific surface. This makes PPS fiber membranes advantageous over flat membranes when used in membrane separations. All these excellent properties make the PPS fiber membrane have great application prospects in the energy and environment field under extreme environments such as high temperatures, strong acids, and alkalis. However, the thermostability and corrosion resistance of PPS also hinder the preparation of PPS fibers and their membranes. Strong corrosion resistance makes PPS difficult to dissolve at room temperature, and thus, the preparation of PPS fiber can only use melt spinning. High-temperature resistance makes PPS fiber preparation temperature much higher than that of the general polymer materials. Furthermore, the melt viscosity of PPS is high, causing it to oxidize easily at high temperatures. Difficulties in the preparation process are one of the major reasons for limiting the development of PPS fiber membranes.

In order to promote the development of PPS fiber membranes and to meet the current demand for separation membranes in the energy and environmental applications, it is imperative to understand their preparation methods and their relevance to different applications. In this paper, four major preparation methods of PPS fiber membranes are described in detail, including two methods of directly preparing PPS fiber membranes (melt-blown spinning and melt electrostatic spinning) and two methods of indirectly preparing PPS fiber membranes (wet papermaking and weaving). Moreover, the applications of PPS fiber

membranes prepared by these four preparation methods mentioned above are discussed in detail in the energy and environmental fields. This paper guides future research on the relationship between the preparation methods and their corresponding applications.

PPS FIBER

The development history of PPS fiber

PPS was first discovered in 1888 by Charles Friedel and James Mason Crafts as a byproduct^[18]. In 1968, Phillips Petroleum Company pioneered the synthesis of linear PPS resins and named the technique the Phillips method or sodium sulfide method. This method was then successfully industrialized by the company in 1973. It successfully developed fiber-grade PPS resin in 1979 and achieved industrial-scale production of PPS fiber staple in 1983, naming the product of “Ryton”. Since then, the company has had a monopoly on the PPS resin and fiber industry. However, the monopoly persisted until 1985, when the patent protection expired. Subsequently, Toray Company and Toyo Spinners Company independently developed their PPS fiber products. In the 21st century, Toray Company acquire the PPS staple fiber business of Fibers & Yarns Company, becoming the world’s largest supplier of PPS fibers. Due to the complex and intricate process of PPS fiber production, many companies in this field have either merged or ceased operations. The timeline of PPS fiber development history is shown in [Figure 1](#).

Properties of PPS fiber

Corrosion resistance

PPS is one of the most corrosion-resistant polymer materials, with a resistance level that is almost equal to that of polytetrafluoroethylene (PTFE)^[19]. It is virtually insoluble in any solvent at temperatures as high as 200 °C^[20]. This inherent chemical resistance allows it to withstand a range of acidic and alkaline substances while maintaining its tensile strength. Wang *et al.* examined the acid resistance properties of PPS fibers by treating them with hydrochloric acid and sulfuric acid^[21]. Notably, these fibers were brittle and turned into yellow solids only when subjected to acid concentrations as high as 6 mol.

High-temperature resistance

PPS fibers can be used continuously at temperatures from 190 to 220 °C^[22]. There is minimal weight loss, or none at all, in both air and nitrogen atmospheres up to 400 °C. However, when the temperature exceeds 100 °C, the degree of oxidation of PPS fibers will increase dramatically with the increase in temperature^[23]. Consequently, many industrial applications that involve high-temperature exhaust from factories, such as dust filter bags, incorporate antioxidants to improve the oxidation resistance of PPS fibers^[24].

Flame retardancy

PPS is structurally stable and has a flame-retardant element, sulfur, which gives PPS fibers an ultimate oxygen index of 34. The combustion rate and smoke production of fibers are remarkably low, and the flame extinguishes naturally upon removal. Remarkably, PPS fibers achieve excellent flame retardant properties without the addition of any flame retardants^[25].

Dielectric performance

PPS fibers exhibit a dielectric constant ranging from 3.9 to 5.1 and a breakdown strength between 13 and 17 kV mm⁻¹. These characteristics render PPS fibers excellent electrical insulators^[26]. Even in demanding conditions characterized by high temperatures, pressures, and frequencies, these fibers maintain their superior electrical insulation capabilities^[17].

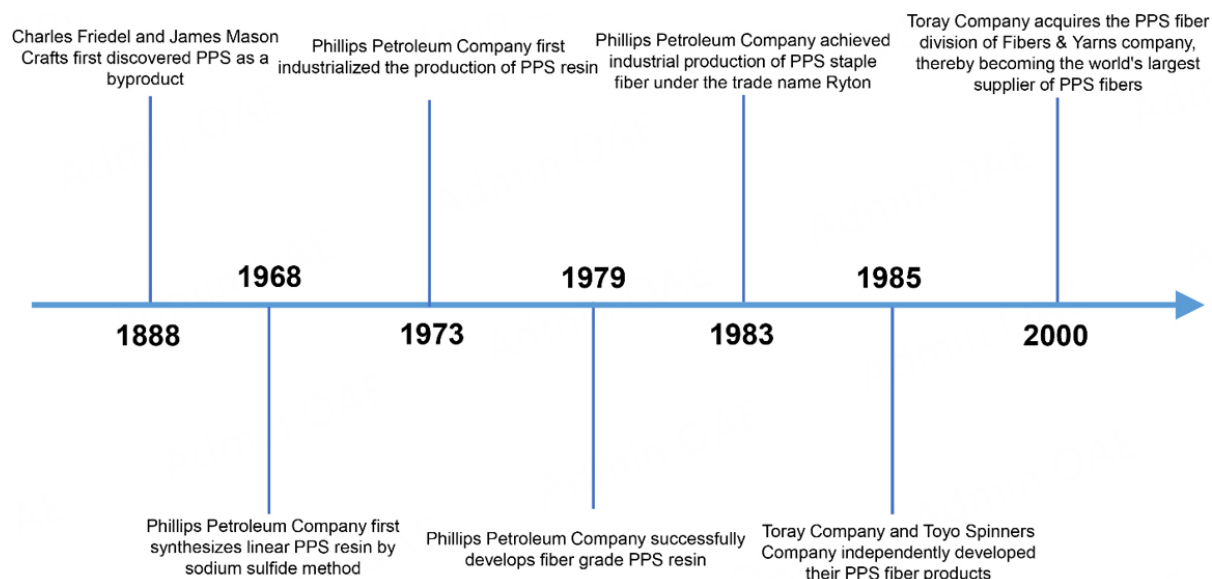


Figure 1. The timeline of PPS fiber development history.

Preparation method of PPS fiber

Due to their resistance to dissolution at room temperature, the major preparation method of PPS fibers is melt spinning^[27]. The main challenge in melt spinning PPS fibers is the high demand for resin feedstock, which requires suitable melt viscosity and relatively high molecular weight^[28]. Inadequate molecular weight and purity of the resin feedstock can lead to thermal cross-linking and tow breakage during spinning and ultimately severely affect fiber properties^[29-31]. Normal injection molding grade PPS resins have a high melt viscosity and cannot be used directly for spinning. Therefore, the development of low-viscosity PPS resins tailored for spinning is a crucial facet in augmenting PPS fiber quality^[28]. In addition, the cooling and crystallization process of the melt is also an essential part of PPS fiber preparation. After extrusion from the spinneret through screw-driven efforts, the PPS melt requires ring blowing technology to promote the cooling crystallization of PPS fibers. After spinning, a series of treatments are necessary to achieve the desired fiber properties, including oiling and multi-stage stretching. The oiling is designed to cool and crystallize the fibers while contributing to fiber bunching, while stretching is used to improve the orientation and mechanical strength of the fibers^[32,33]. The research by Zhang *et al.* delved into the influence of spinning speed on PPS fiber melt spinning, revealing that excessively high speeds can cause fiber breakage and compromise spinnability^[34]. The effect of the post-treatment process on the mechanical properties of PPS fibers was studied by Gulgunje *et al.* Extremely high or low temperatures resulted in a decrease in the mechanical strength of PPS fibers^[35]. A high temperature can lead to the degradation of PPS fibers, while a low temperature could make PPS fibers insufficiently oriented and crystallized.

Industrial production of PPS fibers primarily employs melt spinning, resulting in fiber products primarily composed of cotton-like staple fibers. These fibers are mainly used in the production of high-temperature dust filter bags for the purification of high-temperature exhaust gases in factories. Typically, industrially manufactured PPS fibers exhibit a diameter of approximately 20 μm . However, PPS fiber membranes crafted from fibers of such dimensions can potentially give rise to issues such as substantial thicknesses and overly large pore sizes. Therefore, the development of ultra-fine PPS fibers is one of the important development directions in the PPS fiber spinning industry. This not only puts forward higher requirements for PPS resin raw materials but also requires the improvement of spinning process equipment and conditions.

PREPARATION METHODS OF PPS FIBER MEMBRANES

Melt-blown spinning

Melt-blown spinning is a distinct subtype of melt spinning. In this technique, the polymer melt is extruded through a capillary tube, accompanied by the introduction of compressed air on both sides of the tube. The fractured end of the compressed air influences the polymer melt, drawing it into a microfiber network. Simultaneously, a rotating roller is positioned beneath to collect the ejected fiber web^[36,37] [Figure 2A]. The process of melt-blown spinning requires a specific viscosity of the polymer melt. If the viscosity is too high, it can impede successful draft molding under high-pressure air conditions. Due to the high viscosity of PPS melt and its vulnerability to thermal oxidation at elevated temperatures, producing PPS fiber membranes through melt-blown spinning presents a formidable challenge. To address these challenges, Hu *et al.* undertook the screening of high melt index PPS resins tailored for melt-blown spinning, culminating in the successful production of PPS fiber membranes with diameters ranging from 2 to 5 μm ^[38]. Hu *et al.* further explored the influence of temperature on PPS melt-blown spinning, revealing that low temperatures hinder PPS melt flow, while higher temperatures trigger premature oxidative denaturation and spinneret clogging. Experiments have shown that 330-350 °C is the optimal temperature range for melt-blown spinning of PPS fibers, which is obviously higher than the spinning temperature of ordinary PPS fibers^[38]. Yu *et al.* prepared melt-blown PPS fiber membranes with fiber diameters in the range of 2-6 μm [Figure 2B and C] by screening the resin melt viscosity and improving the spinning equipment and process^[39].

The melt-blown spinning technique facilitates the rapid preparation of PPS fiber membranes. However, due to the high viscosity of PPS melt, achieving melt-blown spinning for PPS fiber membranes necessitates elevated technical prerequisites. Currently, there is no fully developed technology for preparing PPS fiber membranes via melt-blown spinning. Furthermore, due to the inherent randomness associated with melt-blown spinning, the resultant fiber membranes tend to exhibit substantial pore sizes. This characteristic substantially restricts its direct applicability in certain membrane separation contexts.

Melt electrostatic spinning

Electrostatic spinning is a technique that involves extraction of a polymer solution or melt from a syringe and then stretching into nanofibers under the action of a high-voltage electrostatic field [Figure 2D]^[40-42]. This technique enables the direct preparation of nanoscale fiber membranes. One of the most notable developments in this area is melt electrostatic spinning, which employs melt stretching and cooling formation directly under a high-voltage electric field^[43]. This approach circumvents the solvent-related contamination associated with traditional solution electrostatic spinning^[44]. However, unlike solutions, the high viscosity of melts makes it necessary to have higher high-voltage electrostatic fields in order to draw them into nanofibers, which puts higher demands on the equipment for electrostatic spinning. This technology is capable of preparing nanofibers from some polymers (PE, PTFE, *etc.*) that are insoluble at room temperature^[45]. Melt electrostatic spinning offers a rapid and environmentally friendly method for preparing these polymers into nanofiber membranes.

Due to the indissolubility of PPS at room temperature, PPS nanofibers can only be spun by melt electrostatic spinning. Due to the heightened viscosity exhibited by PPS melt during melt electrostatic spinning, An *et al.* resorted to blending PP and PPS to enhance melt fluidity. By optimizing the melt electrostatic spinning process, they successfully prepared PPS fiber membranes with an average fiber diameter of 4.12 μm ^[46]. Further employing the melt differentiation technique within melt electrostatic spinning, Chen *et al.* achieved a PPS fiber membrane boasting an average fiber diameter of 1.28 μm [Figure 2E]^[47]. In another approach, Fan *et al.* introduced inert gas during the melt electrostatic spinning process to mitigate thermal oxidation of PPS at elevated temperatures^[48]. The resultant PPS fiber membrane displayed a fiber diameter of less than 8 μm and commendable tensile strength [Figure 2F]. Kou *et al.*

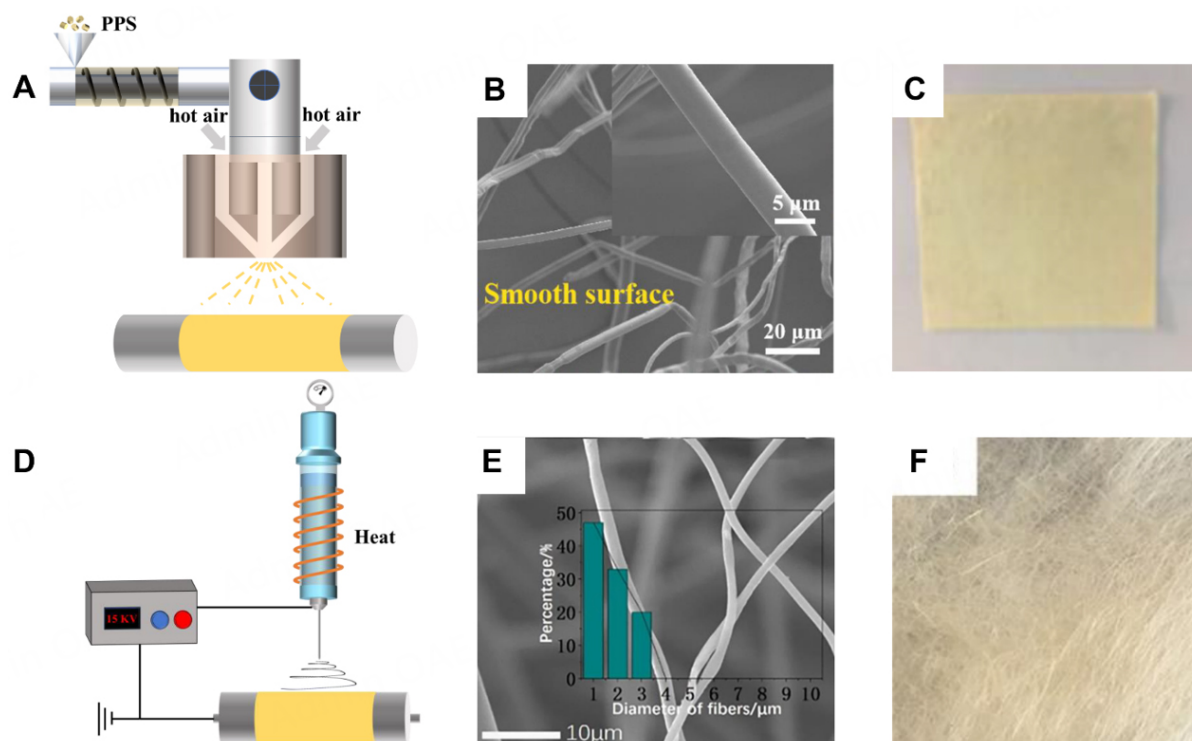


Figure 2. (A) Schematic of melt-blown spinning. (B) SEM of PPS melt-blown fiber membrane. (C) Photograph of PPS melt^[39]. (D) Schematic of melt electrostatic spinning. (E) SEM of PPS melt electrostatic spinning fiber membrane^[47]. (F) Photograph of PPS melt electrostatic spinning fiber membrane^[48].

adopted an alternative route, employing polyvinyl alcohol (PVA) as a sacrificial template and polyacrylonitrile (PAN) as a carrier substrate to form PPS composite nanofiber membranes via solution electrostatic spinning^[49]. Subsequent sintering and removing of PVA caused the PPS particles to melt into fibers, while PAN transitioned into a more stable ring-bound structure during sintering.

Melt electrostatic spinning enables direct preparation of ultra-fine PPS fiber membranes. However, this method necessitates the use of high-voltage electric fields, leading to considerable energy consumption. Furthermore, the yield achieved through melt electrostatic spinning remains limited. This technique also remains largely within the realm of laboratory research, with significant strides required before its practical implementation for production.

Wet papermaking

Wet papermaking is a well-established material preparing technology with a history spanning thousands of years. First, fibers are broken down into pulp (a mixture of fiber and water), which is then dispersed evenly in water. After filtration, the dispersed fibers coalesce to prepare wet paper, which is then dried and pressed to prepare the final paper product [Figure 3A]^[50]. In modern iterations, the range of papermaking raw materials has expanded beyond traditional plant fibers, including inorganic and synthetic fibers^[51]. Capitalizing on its attributes such as reduced thickness, favorable wettability, and heightened porosity, paper serves as a versatile fiber membrane in diverse membrane separation domains. However, producing synthetic fiber-based paper differs from the conventional practice of using plant fibers. Synthetic fibers, which are almost universally hydrophobic, present challenges in achieving uniform dispersion within water. To overcome these challenges, the incorporation of dispersants is necessary to facilitate even dispersion. As

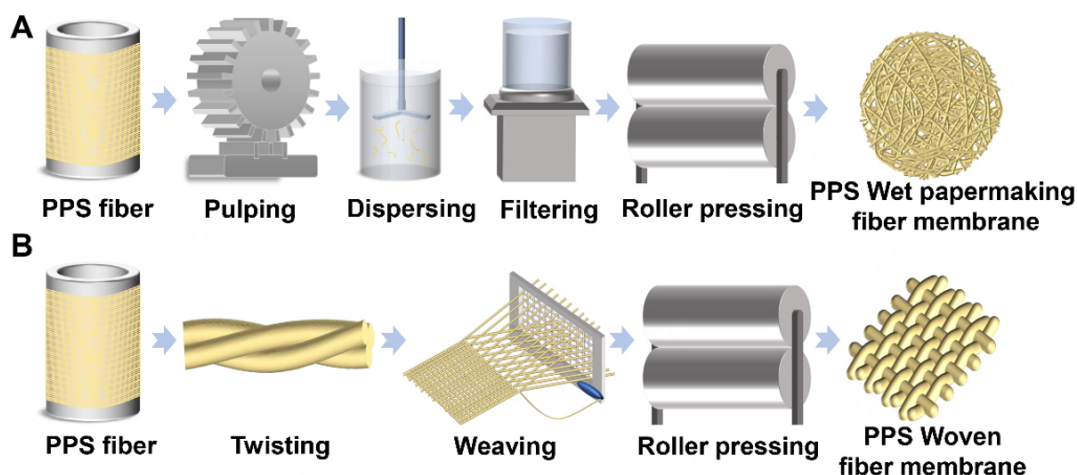


Figure 3. (A) Process of wet papermaking. (B) Process of weaving.

synthetic fibers remain free in water, swift filtration can lead to uneven paper preparation. The strength of wet and dry paper made from synthetic fibers is inherently limited due to the lack of inherent bonding. Therefore, high-temperature rolling technology is necessary to prepare synthetic fiber paper with excellent mechanical properties. High-temperature rolling results in thermal cross-linking of the synthetic fiber paper, thereby increasing its mechanical strength^[52].

Synthetic fibers used in wet papermaking are mainly staple fibers and fiber pulp. The staple fibers are usually only a few millimeters in length. High-performance synthetic fibers, such as PPS, do not lend themselves to conventional precipitation-based pulp formation due to their resistance to dissolution at room temperature. Therefore, PPS fibers must be made into fiber pulp by mechanical pulping. Furthermore, ordinary PPS fibers, due to their large fiber diameter and hydrophobic surface, do not lend themselves well to wet papermaking. Preparing fiber membranes directly through wet papermaking utilizing these ordinary PPS fibers results in pronouncedly large pore sizes and thicknesses. Additionally, since PPS fibers lack inherent bonding, laminating them with fibers endowed with bonding strength can achieve fiber membranes with robust mechanical strength^[53,54]. Zhu *et al.* used melt-blown PPS nonwoven fabrics with fiber diameters averaging around 2–6 μm as raw materials, combining them with aramid nanofibers (ANFs) to create a PPS/ANFs composite fiber membrane, 50 μm thick^[55]. This composite fiber membrane had a porosity of 65.9% and a tensile strength of 9.8 MPa. They further incorporated cellulose, an environmentally friendly, hydrophilic, chemically stable, and thermally stable nanofiber, along with PPS fibers to prepare a fiber membrane^[53,54]. The abundance of cellulose nanofibers helps regulate the pore size structure of the PPS fiber membrane. Inherent hydrogen bonding in cellulose enhances the mechanical strength of the composite fiber membrane. Yu *et al.* utilized ultrafine PPS fibers with an average fiber diameter of 1 μm obtained through the island spinning method^[56]. By amalgamating this fiber material with nano-sized glass fibers through the papermaking technique, they achieved a PPS composite fiber membrane 34 μm thick, marked by a porosity of 65.4% and a tensile strength of 22.2 MPa.

As a promising approach to industrialization, wet papermaking holds significant potential for the preparation of PPS fiber membranes. However, the majority of PPS fibers are in the form of cotton-like staple fibers, featuring lengths of 5–6 cm. These fibers are not conducive to wet papermaking practices. Therefore, there is a pressing need to develop PPS staple fibers or pulp that align with the prerequisites of wet papermaking.

Weaving

Weaving is the formation of two-dimensional and even three-dimensional structures based on one-dimensional yarns interwoven^[57]. This regular interlocking of fibers leads to robust mechanical properties in woven fiber membranes. The transformation from individual fibers to woven fiber membranes encompasses stages including twisting (combining multiple bundles of fibers into a single bundle), warping (rotating a bundle of fibers in a spiral), drawing-in (Fiber bundles with helical structures are shaped by heating), and weaving [Figure 3B]^[58]. High-temperature filter bags made of woven PPS fibers have been widely used in factories for dust removal and filtration of high-temperature exhaust gases. Specific applications may also necessitate additional processes such as hot pressing, surface coating, and modifications of the woven fiber membrane. Both short and long PPS fibers can be employed to fabricate woven fiber membranes. Long fiber membranes generally exhibit higher breaking strengths, whereas short fiber membranes tend to possess greater porosity. Nevertheless, the average pore size of both membrane types exceeds 50 μm , which proves excessively large for most membrane separation purposes.

To address the challenge of overly large pore sizes in woven fiber membranes, current research leans towards composite membranes constructed on the foundation of woven fiber networks with internal and surface coatings of inorganic oxides. Leveraging the fiber woven network as a substrate effectively bolsters the mechanical robustness of the composite membrane, thereby extending the operational lifetime of the membrane^[59,60]. A case in point is the Zirfon membrane, which employs a woven network of PPS fibers coated with ZrO_2 and polysulfone (PSU)^[61]. These Zirfon membranes are applied in alkaline water electrolysis (AEL). This organic-inorganic composite separator combines the toughness of polymer materials with the small pore size and hydrophilicity of inorganic ceramic materials.

In general, ordinary PPS woven fiber membranes contend with notable pore sizes and substantial thickness. Remedying these challenges requires enhancements spanning the fiber diameter and weaving process. Furthermore, the primary concern associated with composite PPS woven fiber membranes that utilize a PPS fiber woven network as a substrate lies in achieving strong bonding between the substrate and coating layer. Insufficient bonding could significantly curtail the operational lifespan of such composite woven fiber membranes.

ENERGY APPLICATIONS

Lithium-ion batteries

Lithium-ion batteries are a crucial energy storage technology in contemporary applications such as mobile devices and electric vehicles^[62]. They consist of cathode, anode, electrolyte, and separator components [Figure 4A]. The separator serves two purposes: it separates the cathode and anode to avoid short circuits and ensures the transfer of ions between the cathode and anode^[63]. The porosity, electrolyte wettability, and heat resistance of separators significantly influence the capacity, cycling performance, and safety of lithium ions. Lithium-ion battery separators can be classified into microporous, nonwoven, electrostatic spinning, surface-modified, and composite separator variants^[64]. Commercialized lithium battery separators typically feature polyolefin-based microporous separators derived from PP or PE, which excel in mechanical properties, corrosion resistance, and affordability. However, the limited electrolyte wettability, subpar flame retardancy, and notable thermal shrinkage of polyolefin separators precipitate safety concerns in assembled lithium-ion batteries^[65]. The rapid charging and discharging of lithium-ion batteries can lead to overheating. Polyolefin separators are thermally unstable and susceptible to shrinkage in extreme environments, potentially culminating in battery short-circuiting. Such a short circuit could trigger uncontrollable internal chemical reactions, liberating excessive heat and potentially resulting in fires or explosions. This is evidenced by instances such as battery fires in Tesla electric cars, Samsung cell phones, and Boeing airplanes^[66]. The PPS fiber has excellent thermal stability, and its working temperature can reach 200 $^{\circ}\text{C}$.

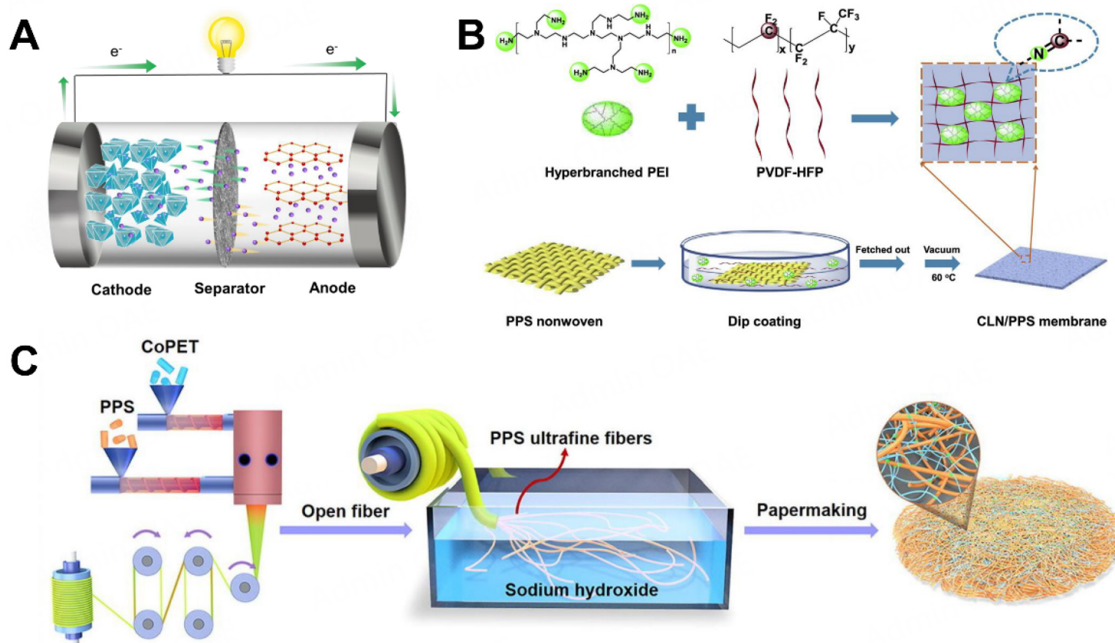


Figure 4. (A) Schematic of lithium-ion battery. (B) Preparation of CLN/PPS membrane and construction procedure for cross-linked polymer electrolyte networks (CLN)^[70]. (C) Preparation schematic illustration of PPS sea-island ultrafine fiber and its composite membrane^[56].

This ensures the resistance of separators to shrinking during overheating, thereby mitigating safety concerns related to short circuits and overheating. Moreover, fiber membranes offer higher porosity and a more uniform pore structure, diminishing the formation of lithium dendrites when used as separators, enhancing cycling and safety attributes of lithium-ion batteries^[67]. Therefore, the utilization of PPS fiber membranes as lithium battery separators not only improves battery cycling performance but also prevents overheating and short-circuit safety issues.

In the realm of researching PPS fiber membrane applications in lithium-ion batteries, two primary membrane types emerge: melt-blown fiber membranes and wet papermaking fiber membranes. Melt-blown processing facilitates the rapid preparation of PPS fiber membranes with diminutive fiber diameters. However, the inherent randomness of this process leads to uneven pore size distribution in PPS fiber membranes, rendering them unsuitable for direct application as lithium battery separators and prone to self-discharge and erratic current distribution^[68]. To address this issue, a physical coating approach is pivotal in optimizing the pore size and distribution of PPS fiber membranes. Luo *et al.* coated melt-blown PPS fiber membranes with poly(vinylidene fluoride-hexafluoropropylene) (PVDF-HFP) and inorganic nanoparticles SiO₂ to refine membrane pore characteristics and enhance electrolyte wettability on the surface^[69]. Alternatively, a cross-linked polymer network could be generated on the surface of melt-blown PPS fiber membranes by reacting PVDF-HFP with hyperbranched polyethylenimine (PEI), thereby increasing the electrolyte absorption capacity and ionic conductivity of membranes while enhancing mechanical strength [Figure 4B]^[70]. However, melt-blown PPS fiber membranes still have a high thickness, which leads to increased impedance in lithium-ion batteries, reducing capacity and cycling performance.

On the contrary, wet papermaking is achieved through the uniform dispersion of fibers in water to achieve a uniform stacking of fibers into a membrane, which ultimately forms a superior pore size structure. However, these fibers remain only interlinked by crossing each other, resulting in relatively modest

mechanical strength. To address this concern, ongoing research is focusing on two mechanisms: the formation of a polymer cross-linking network on the PPS fiber membrane surface^[71,72] and the integration of other fibers in composite wet papermaking membranes. Composite papermaking fibers encompass ANFs^[55], cellulose fibers (CFs)^[53,54], and glass fibers^[56]. The excellent thermal stability of ANFs makes ANFs/PPS composite membranes virtually heat-shrinkage free at 200 °C [Figure 5A-D]. The nanoscale fiber structure makes ANFs/PPS composite membranes have high porosity and small pore size, which makes the surface of the membrane well wettable for the electrolyte [Figure 5E-H]. ANFs are also excellent flame-retardant fibers, and the composite with PPS fibers obtains a good flame-retardant effect [Figure 5I and J]. In addition, the high strength of aramid and the bonding between fibers greatly enhance the mechanical strength of ANFs/PPS composite membranes, which reaches 9.8 MPa. CFs are transformed into abundant nanofibers upon pulping, boasting augmented mechanical strength through chemical bonding. The hydroxyl groups on the CF surface engage in hydrogen bonding with the electrolyte, thereby ameliorating membrane wetting behavior^[73]. Zhu *et al.* used a wet papermaking process to prepare a natural CFs/PPS fiber composite membrane with mechanical strength of 20.52 MPa, which was superior to the transversal direction strength of the Celgard 2400 separator (10.44 MPa) [Figure 5K]^[53]. A glass fiber, being an inorganic fiber, differs from polymer fibers in its characteristics. The combination of glass and PPS fibers in a composite wet papermaking membrane necessitates careful consideration of the interfacial bond between these two types of fibers. Yu *et al.* prepared ultra-fine PPS fibers with an average fiber diameter of 1 μm by island spinning^[56]. These ultrafine PPS fibers were then combined with nano glass fibers via a silane coupling agent, preparing a membrane through the wet papermaking process [Figure 4C]. The strong bond between the silane coupling agent-treated PPS fibers and the glass fibers resulted in a composite fiber membrane with a tensile strength of 22.2 MPa [Figure 5L]. Additionally, the diameter of PPS fibers fabricated by island spinning is small (1 μm), and the PPS fiber membrane prepared from it has uniform and small pores. The Li|separator|Li symmetric cells show excellent electrochemical performance and stable voltage plateau after cycling at 2.5 mA cm⁻² for 1,000 h [Figure 5M]. The uniform pore structure results in a more uniform deposition of lithium metal, which, in turn, reduces the growth of lithium dendrites and improves the overall cycle stability of the battery. The capacity retention rate is up to 95.6% even after 200 cycles at 1 C [Figure 5N]. A comprehensive overview of the research on PPS fiber membranes in lithium-ion battery applications is provided in Table 1.

In summation, PPS fiber membranes prepared from the wet papermaking process exhibit small and distributed pore sizes compared to those prepared by the melt-blown spinning. With ongoing advances in synthetic fiber for wet papermaking, the prospects of large-scale production and actual deployment of wet papermaking PPS fiber lithium-ion battery separator membranes are promising. Despite their promising properties, PPS fiber membranes are currently more expensive than the commonly used PP separators in lithium-ion batteries. In comparison to aramid separators, PPS fiber membranes are more affordable, but their mechanical property is not enough. This highlights the need for further research and development to improve the cost-effectiveness and high-performance PPS fiber membranes, making them a more attractive option for use in various applications.

Alkaline water electrolysis

Hydrogen energy is regarded as the ideal clean energy source in the future, and water electrolysis for hydrogen production is considered a clean and environmentally friendly method. There are four significant techniques for hydrogen production through water electrolysis: AEL, polymer electrolyte membrane water electrolysis (PEMWE), anion exchange membrane water electrolysis (AEMWE), and solid oxide water electrolysis (SOEC)^[74]. Among these, AEL is currently the most technologically mature and least expensive^[75]. The separator plays a crucial role in AEL, serving two primary functions: (1) Enabling the free movement of ions within the electrolyzer. The interfacial affinity between separators and electrolytes has a

Table 1. Summary of PPS fiber membranes in lithium-ion battery applications

Materials	Preparation method	Thickness (μm)	Porosity (%)	Electrolyte uptake (%)	Tensile strength (MPa)	Dimensionally stability temperature ($^{\circ}\text{C}$)	Ion conductivity (mS cm^{-1})	Cycling performance	Refs.
PVDF-HFP/SiO ₂ -PPS	Dip-coating and melt-blown spinning	114	57.3	230.1	4.9	250 $^{\circ}\text{C}$, 0.5 h no shrinkage	1.02	85.1% after 50 cycles at 0.2 C	[69]
PVDF-HFP/PEI-PPS	Dip-coating and melt-blown spinning	95	65	197	11.35	200 $^{\circ}\text{C}$, 0.5 h no shrinkage	0.52	91.8% after 100 cycles at 0.5 C	[70]
PVDF-HFP/PEI/SiO ₂ -PPS	Dip-coating and papermaking	49	71	254	9.9	250 $^{\circ}\text{C}$, 1 h no shrinkage	0.69	98% after 100 cycles at 0.2 C	[71]
PDMSDGE/PVDF-HFP/PEI-PPS	Dip-coating and papermaking	55	70	230	19.9	200 $^{\circ}\text{C}$, 1 h no shrinkage	0.59	85% after 200 cycles at 0.5 C	[72]
ANFs/PPS	Papermaking	50	65.9	240.7	9.8	200 $^{\circ}\text{C}$, 0.5 h no shrinkage	1.43	92% after 100 cycles at 0.5 C	[55]
CFs/PPS	Papermaking	/	61.1	259.6	20.52	200 $^{\circ}\text{C}$, 0.5 h no shrinkage	1.26	90.3% after 100 cycles at 0.5 C	[53]
BC/PPS	Papermaking	60	62.7	216.2	-18	200 $^{\circ}\text{C}$, 0.5 h no shrinkage	-1.55	91.3% after 100 cycles at 0.2 C	[54]
GNF/PPS	Papermaking	34	65.4	270.7	22.2	250 $^{\circ}\text{C}$, 0.5 h no shrinkage	1.43	95.6% after 200 cycles at 1 C	[56]

PDMSDGE: Polydimethylsiloxane; ANFs: aramid nanofibers; CFs: cellulose fibers; BC: bacteria cellulose; GNF: glass nanofibers.

direct impact on the internal resistance of the electrolyzer, thus influencing the energy consumption and overall efficiency. Furthermore, a hydrophobic separator can lead to hydrogen and oxygen accumulation on either side, hampering ion transfer efficiency and gas purity at the outlet; and (2) Segregating the hydrogen and oxygen produced in the electrolyzer. The gas-tight property of the separator is crucial in maintaining gas purity at the outlet, also affecting the safety of the electrolyzer due to the differential pressure fluctuations during operation^[75]. To reduce the internal resistance of the electrolyzer in the industry, the electrode net and separator are superimposed simultaneously. The schematic of this zero-gap electrolyzer is shown in [Figure 6A](#).

Initially, asbestos was used as a separator in AEL. However, the dissolution and chemical instability of asbestos in high-temperature alkaline electrolytes led to shortened lifespans^[76]. Moreover, asbestos is categorized as a carcinogenic substance and has been prohibited by the International Health Organization^[77]. PPS fibers have several attractive properties, such as impressive mechanical properties, robust alkali resistance, and outstanding electrochemical traits. These fibers can effectively replace asbestos in conventional AEL separators by being prepared into woven fabrics. However, the hydrophobicity of the PPS woven fabric and the large pores created by the weave result in high hydrogen permeability and energy consumption in the electrolyzer. Therefore, PPS woven fiber membranes require further modifications to enhance their hydrophilicity and airtightness^[78].

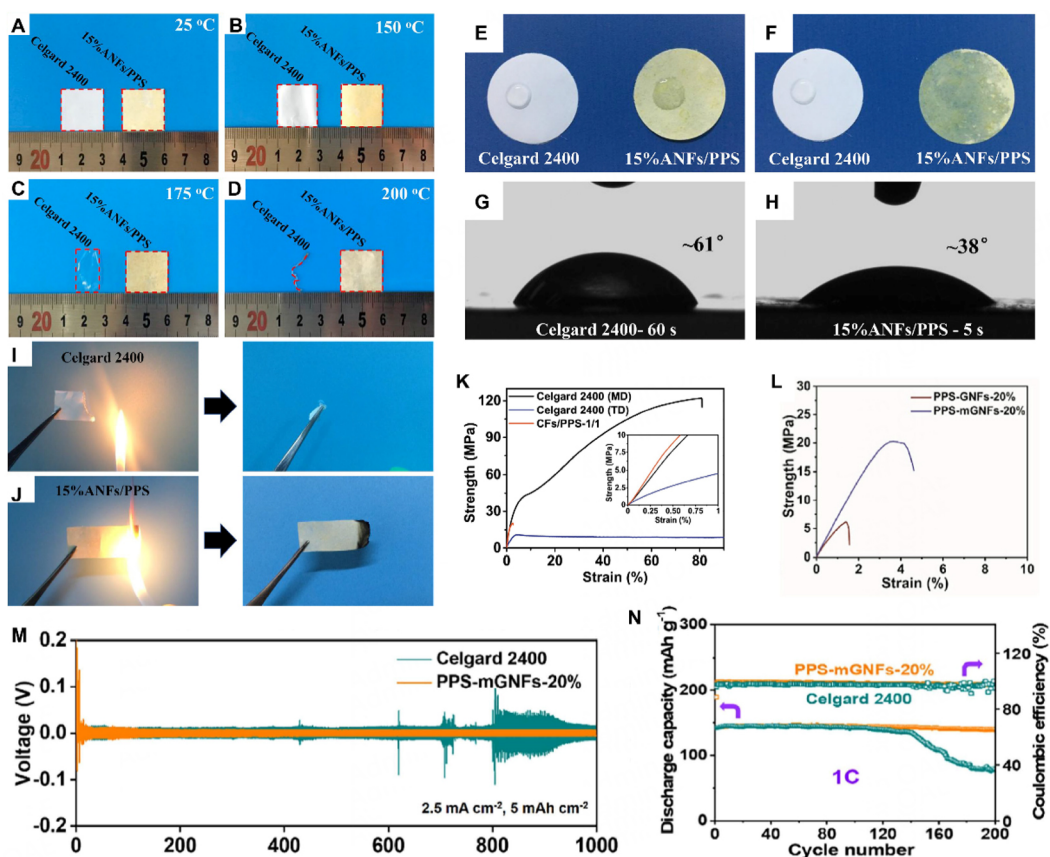


Figure 5. Photographs of Celgard 2400 and 15% ANFs/PPS membrane before and after heat treatment at different temperatures for 30 min: room temperature (A), 150 °C (B), 175 °C (C), and 200 °C (D). Wettability images of Celgard 2400 and 15% ANFs/PPS membrane: The images of the liquid electrolyte just (E) and after 30 s (F) dripped to the surface. Contact angle images of the Celgard 2400 separator (G) after dripping 2 μ L liquid electrolyte for 60 s and the ANFs/PPS membrane (H) after dripping 2 μ L liquid electrolyte for 5 s. Ignition tests of Celgard 2400 (I) and 15% ANFs/PPS membrane (J)^[55]. (K) The stress-strain curves of Celgard 2400 separator in machine direction (MD) and transversal direction (TD) and CFs/PPS-1/1 separator^[53]. (L) The stress-strain curve of PPS-GNFs-20% and PPS-mGNFs-20%. (M) Electrochemical performance of cells with Celgard 2400 and PPS-mGNFs-20% membrane. Voltage profiles of the Li|separator|Li symmetric cells at 2.5 mA cm⁻², 5 mAh cm⁻². (N) Cycling performance of the cells^[56]. Celgard 2400: A commercially available PP lithium-ion battery separator; Li|separator|Li symmetric cells: a battery system for testing the long cycle stability of lithium-ion batteries.

To enhance the hydrophilicity and airtightness of PPS fiber woven membranes, two primary methods have been reported: surface modification [Figure 6B] and inorganic nanoparticle coating [Figure 6C]. Surface modification techniques include cross-linking^[79], sulfonation^[80], and grafting^[81]. Inorganic nanoparticles include ZrO₂^[82,83], TiO₂^[84], and CeO₂^[85]. The direct surface modification of PPS fiber woven membranes offers a convenient and cost-effective avenue. For instance, sulfonation is the enhancement of hydrophilicity by introducing sulfonic acid groups to the surface of PPS fibers. Sun *et al.* investigated the impact of sulfonation and hot roller rolling on PPS fiber woven membranes, revealing the enhanced alkaline solution absorption through sulfonation and improved airtightness *via* hot roller pressing^[86,87]. However, this surface modification compromises fiber integrity, resulting in reduced mechanical properties and longevity of the membrane. The surface modification cannot fundamentally change the poor hydrophobicity and airtightness of PPS fiber woven membranes. The selectivity, permeability, and mechanical properties of the composite separator could be maximized by preparing a composite membrane consisting of one or more membranes on a porous substrate^[88]. Therefore, a composite membrane with PPS fiber woven mesh as the substrate coated with inorganic particles may be necessary to achieve the desired hydrophilicity and

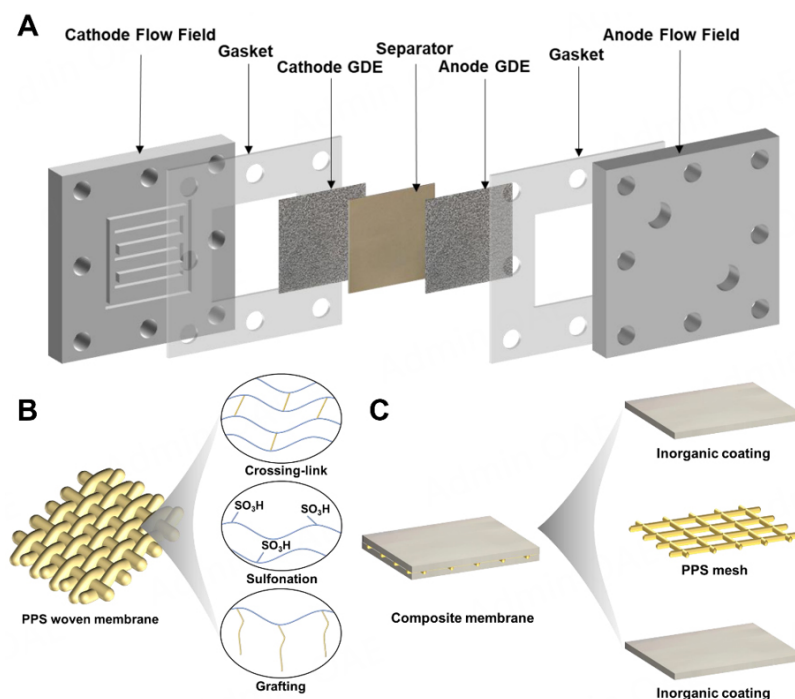


Figure 6. (A) Schematic of zero-gap electrolytic cell. (B) Surface modification of PPS woven membrane. (C) Sandwich structure of composite separator.

airtightness. This approach would combine the benefits of PPS fibers with the superior hydrophilicity and airtightness provided by the inorganic nanoparticles.

The Zirfon membrane developed by Agfa (Belgium) is a typical example of composite separators. The coating consists primarily of hydrophilic ZrO_2 nanoparticles and PSU^[89]. The Zirfon membrane exhibits a sandwich-like structure, featuring distinct pore size regions: a 30 nm pore formed by ZrO_2 nanoparticles and a larger pore of over 1 μm formed by the PSU network^[90]. In Lee *et al.* from the Korea Energy and Hydrogen Research Institute explored the ZrO_2 to PSU ratio in Zirfon membranes^[91]. Notably, 85 wt% of ZrO_2 nanoparticles in the Zirfon membrane had the lowest ohmic resistance (approximately $0.2 \Omega \text{ cm}^2$), while 75% wt% of ZrO_2 nanoparticles achieved optimal gas tightness, resulting in a low hydrogen permeability ($4 \times 10^{-12} \text{ mol bar}^{-1} \text{ s}^{-1} \text{ cm}^{-1}$). Although the Zirfon membranes display low ohmic resistance and hydrogen permeability, ZrO_2 nanoparticles are not strongly bound to PSU. Qiu *et al.* further introduced polyvinylpyrrolidone (PVP) to the coating slurry to create Zirfon separators with reduced ohmic resistance ($0.1 \Omega \text{ cm}^2$), minimal hydrogen permeability ($0.2 \times 10^{-12} \text{ mol bar}^{-1} \text{ s}^{-1} \text{ cm}^{-1}$), and exceptional durability (stable operation under 80 °C and 30 wt% KOH solution for 300 h) through adjustments to solidification bath temperature and PVP quantity^[60]. The critical factors affecting separator ionic conductivity and gas resistance are the electrical conductivity and particle size of inorganic nanoparticles. Therefore, Ali *et al.* employed zirconia toughened alumina as an inorganic filler to further enhance the electrical conductivity of ZrO_2 and reduce the ohmic resistance of the separator to $0.15 \Omega \text{ cm}^2$ ^[92]. Lee *et al.* also compared the effect of CeO_2 nanoparticles with different particle sizes on composite separators^[85]. Scanning electron microscope (SEM) of the separator sections showed that CeO_2 bonded better to the PSU than that of ZrO_2 [Figure 7A]. The 10 nm CeO_2 [Figure 7B] showed a significant aggregation, while 50 nm [Figure 7C] and 100 nm [Figure 7D] CeO_2 were well dispersed. Further characterization revealed that good CeO_2 dispersion was found with a size of $\sim 100 \text{ nm}$. The composite membrane, with relatively small pore size (77 nm), reduced

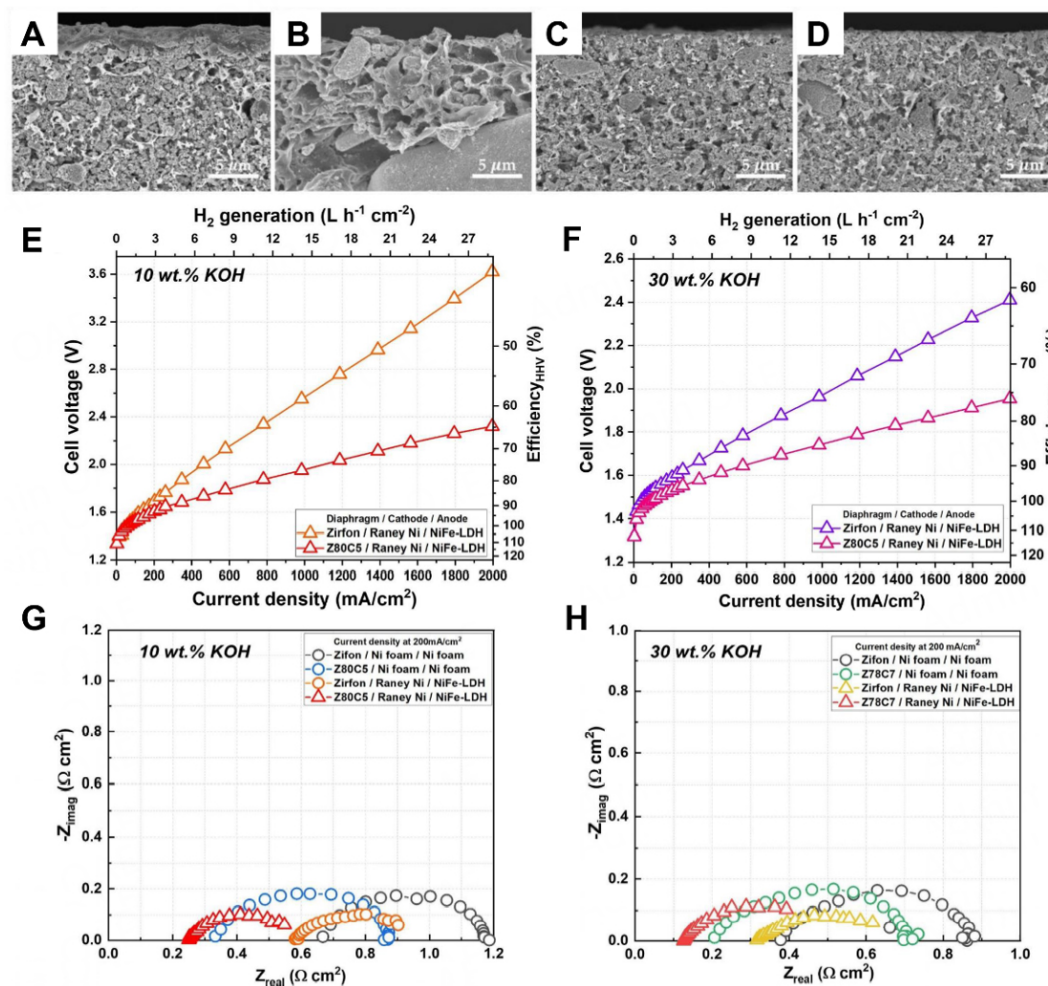


Figure 7. (A) Cross-sectional SEM images of Zirfon. Cross-sectional SEM images of composite membrane of different particle sizes of CeO₂ (B) 10 nm, (C) 50 nm, (D) 100 nm^[85]. Polarization curves (E) Z80C5 in 10 wt% KOH (F) Z80C5 in 30 wt% KOH. Nyquist impedance plots (G) Z80C5 in 10 wt% KOH (H) Z80C5 in 30 wt% KOH. Catalysts: Raney Ni/NiFe-LDH (nickel-iron layered double hydroxide)^[93]. The sample named Z80C5 indicates the separator composed of 80 wt% ZrO₂ and 5 wt% CNCs. The Raney Ni and NiFe-LDH are both commonly used electrode catalyst materials in alkaline water electrolysis.

ohmic resistance ($0.16 \Omega \text{ cm}^2$), and hydrogen permeability ($1.2 \times 10^{-12} \text{ mol bar}^{-1} \text{ s}^{-1} \text{ cm}^{-1}$), surpasses commercial Zirfon membranes. Another innovative approach involved mixing cellulose nanocrystals (CNCs) with ZrO₂ to prepare composite separators with heightened hydrophilicity. This led to diminished ohmic resistance ($0.18 \Omega \text{ cm}^2$) and hydrogen permeability ($4.7 \times 10^{-12} \text{ mol bar}^{-1} \text{ s}^{-1} \text{ cm}^{-1}$) at low electrolyte concentrations (10 wt% KOH)^[93]. The hydrogen generation rate of the electrolyzer is higher for the Z80C5 (membrane composed of 80 wt% ZrO₂ and 5 wt% CNCs) membrane than that of the Zirfon membrane, both at 10 wt% KOH and 30 wt% KOH [Figure 7E and F]. The hydrophilic Z80C5 membrane has a low ohmic resistance compared to the Zirfon membrane in both 10 wt% KOH and 30 wt% KOH [Figure 7G and H]. A comprehensive overview of the research on PPS fiber membranes in AEL applications is provided in Table 2.

While composite separators made with inorganic nanoparticles exhibit lower ohmic resistance and hydrogen permeability than those made of woven PPS fiber membranes, their cost is significantly high. Furthermore, the continuous shedding of inorganic particles from the surface of composite separators due

Table 2. Summary of PPS fiber membranes in alkaline water electrolysis application

Materials	Thickness (μm)	Porosity (%)	Bubble point pressure (bar)	Area resistance (Ω cm ²)	Hydrogen permeability (mol bar ⁻¹ s ⁻¹ cm ⁻¹)	Electrolyte	Refs.
PPS staple fiber membrane	300	73	2.79×10^{-3}	0.191	/	30 wt% KOH	[87]
PPS filament fiber membrane	300	43.8	3.08×10^{-3}	0.159	/	30 wt% KOH	[87]
ZrO ₂ /PSU composite membrane (ZrO ₂ :PSU = 75:25)	478 ± 7	49.3	3.8 ± 0.1	0.35 ± 0.2	4.2×10^{-12}	30 wt% KOH	[91]
ZrO ₂ /PSU composite membrane (ZrO ₂ :PSU = 85:15)	484 ± 7	55.8	1.5 ± 0.1	0.21 ± 0.1	-20×10^{-12}	30 wt% KOH	[91]
ZrO ₂ /PSU/PVP composite membrane	300	/	/	0.1	20×10^{-12}	30 wt% KOH	[60]
CeO ₂ /PSU composite membrane	460 ± 25	46 ± 2	4 ± 0.1	0.16 ± 0.02	1.2×10^{-12}	30 wt% KOH	[85]
ZrO ₂ /PSU/CNCs composite membrane	468 ± 30	41	6.6 ± 0.5	0.18	4.7×10^{-12}	10 wt% KOH	[93]

to prolonged use significantly increases the need for frequent replacements, which can reduce the cost. This makes composite separators uncompetitive in the AEL market. Therefore, reducing the cost of composite separators and improving their service life is the focus of future research on composite separators.

Comparison between lithium-ion battery separators and alkaline water electrolysis separators

The three-dimensional porous structure of PPS fiber membranes makes them highly suitable for use as separators in lithium-ion batteries and AEL. However, there are some important differences between the requirements of these two types of separators. Lithium-ion battery separators demand exceptional thermal stability and good wetting with the different electrolytes. Additionally, it also necessitates a thinner and more uniform pore structure to ensure consistent performance^[94]. On the other hand, AEL separators require not only exceptional thermal stability of the material but also robust chemical stability at high temperatures. Furthermore, the structure must have a sufficient thickness and a very small pore size to prevent gas crossings^[95]. Despite these differences, PPS fibers exhibit both excellent thermal and chemical stability, making them ideal for both types of separators. The versatility of PPS fiber membranes lies in the fact that their thickness and pore size can be achieved by different preparation processes, which makes them a very promising membrane material for the energy field.

ENVIRONMENTAL APPLICATIONS

Air filtration

In recent decades, the rapid development of industry has led to the accumulation of particulate matter (PM) in the air, which has a major impact on human health^[96]. The sources of PM are mainly ammonia, SO_x, NO_x, and other high-temperature corrosive components from power plants, chemical plants, and fossil fuel combustion^[97]. Traditional air filtration polymer membranes (polyester) have poor chemical and thermal stability and are prone to degradation and failure in the harsh environment of high temperatures and strong corrosion. The excellent corrosion resistance and thermal stability of PPS fibers allow separation membranes to have long periods in the harsh environment of high temperatures and corrosion. PPS fibers have a low price compared to other high-temperature and corrosion-resistant high-performance fiber materials (PTFE, polyimide, etc.), which makes them widely used in factory exhaust dust filter bags^[24]. However, PPS fiber dust filter bags still face the problems of low filtration precision, oxidation and thermal cross-linking reaction at high temperatures^[98]. PPS dust filter bags are often woven or spun-bond nonwoven

fabrics, and the fiber diameter is large, resulting in a large filter bag pore size. Moreover, when PPS fibers are at a higher temperature than 100 °C, their oxidation reaction is sharply elevated, especially in the presence of the nitrogen oxides in the factory exhaust gas, resulting in extremely serious oxidation of PPS fibers^[99,100].

For the problems of PPS fiber dust filter bags, the current research is primarily focused on two aspects. One approach is to use the ultra-fine PPS fibers or compose with other ultra-fine fibers to achieve the reduction of pore space, thus improving the filtration capacity. Zhao *et al.* combined homemade melt-blown ultra-fine PPS fibers (diameter < 5 μm) with aramid fibers for wet papermaking to prepare ultra-fine PPS/PPTA (polyterephthaloyl-p-phenylenediamine) composite fiber membranes^[101]. The ultra-fine PPS fibers enhanced the filtration efficiency of the composite fiber membrane, obtaining a filtration efficiency of 89.02% and 99.99% for PM_{0.3} and PM_{2.5}, respectively. Additionally, the addition of aramid fibers further enhances the high temperature and acid/alkali resistance of the PPS composite fiber membrane. A PPS/PPTA composite fiber membrane could maintain a high filtration efficiency for PM_{2.5} and PM_{0.3} after 48 h at 240 °C [Figure 8A], acid treatment [Figure 8B] and alkali treatment [Figure 8C], respectively. Ye *et al.* created a thin sandwich of a network fiber structure between a PPS fiber substrate and an expanded PTFE (ePTFE) membrane by electrostatic spinning^[102]. The gas permeability and dust filtration efficiency of the composite PPS fiber filtration membrane were improved by introducing fibers with different melting temperatures. Without introducing other types of fibers, the PPS fibers easily soften and melt under the temperature and pressure of the hot rollers, leading to clogging of the membrane pores [Figure 8D]. The introduction of fibers with lower melting temperatures than that of the PPS fibers can significantly reduce the pressing temperature and thus increase the gas flux of the composite PPS fiber filtration membrane [Figure 8E]. Additionally, the introduction of fibers with similar melting temperatures to PPS fibers improves the mechanical strength, although it can lead to blockage caused by the co-melting of the two fibers [Figure 8F]. The introduction of fibers with a melting temperature higher than that of PPS fibers can effectively reduce the blockage caused by melting PPS, thus improving air permeability [Figure 8G]. This unique nanofiber composite strategy provides a good reference for various subsequent nanofiber composite PPS fiber filtration membranes. Zhang *et al.* blended ultrafine PPS fibers with conventional PPS fibers as the upper layer of nonwoven needle felt (NWNF) and prepared a composite PPS fiber filter membrane with gradually increasing pore size by lamination^[103]. The gradual increase in pore size structure increased the filtration resistance to some extent [Figure 8H] but significantly improved the filtration efficiency and long-term stability of the composite PPS fiber filtration membrane [Figure 8I]. Although reducing the diameter of PPS fibers or compositing them with other microfibers can significantly enhance the filtration efficiency and lifetime of PPS fiber filter membranes, it still cannot solve the problem of oxidation of PPS fibers at high temperatures, especially in the presence of NO_x and other gases.

Another approach for improving the efficiency of PPS fiber filtration is to load functional materials on the surface of the fiber to achieve high-efficiency filtration of particles or selective adsorption of special gases. Therefore, another focus of research on PPS fiber filtration membranes is the construction of functional materials on the surface of PPS fibers for the removal of gases with high oxidizing properties, such as NO_x. Zheng *et al.* generated nano-flowering manganese dioxide *in situ* on the surface of PPS fiber filtration membranes to achieve a high-efficiency conversion rate of NO by PPS fiber filtration membranes^[104]. Their denitrification rate was as high as 100% at a temperature of 180 °C. However, prolonged use leads to a significant decrease in the activity of the catalyst. Therefore, Zhang *et al.* subsequently prepared a polypyrrol coating layer on the surface of the PPS fiber filter membrane to improve the bonding of the catalyst with the fiber membrane and the catalytic stability of the catalyst^[105]. Luo *et al.* used a hydrothermal method to anchor petal-like Mn₄FeO_x amorphous oxide catalysts onto PTFE/PPS composite filtration membranes^[105]. The synergistic interaction between Fe and Mn promoted the growth of the catalysts on the surface of the

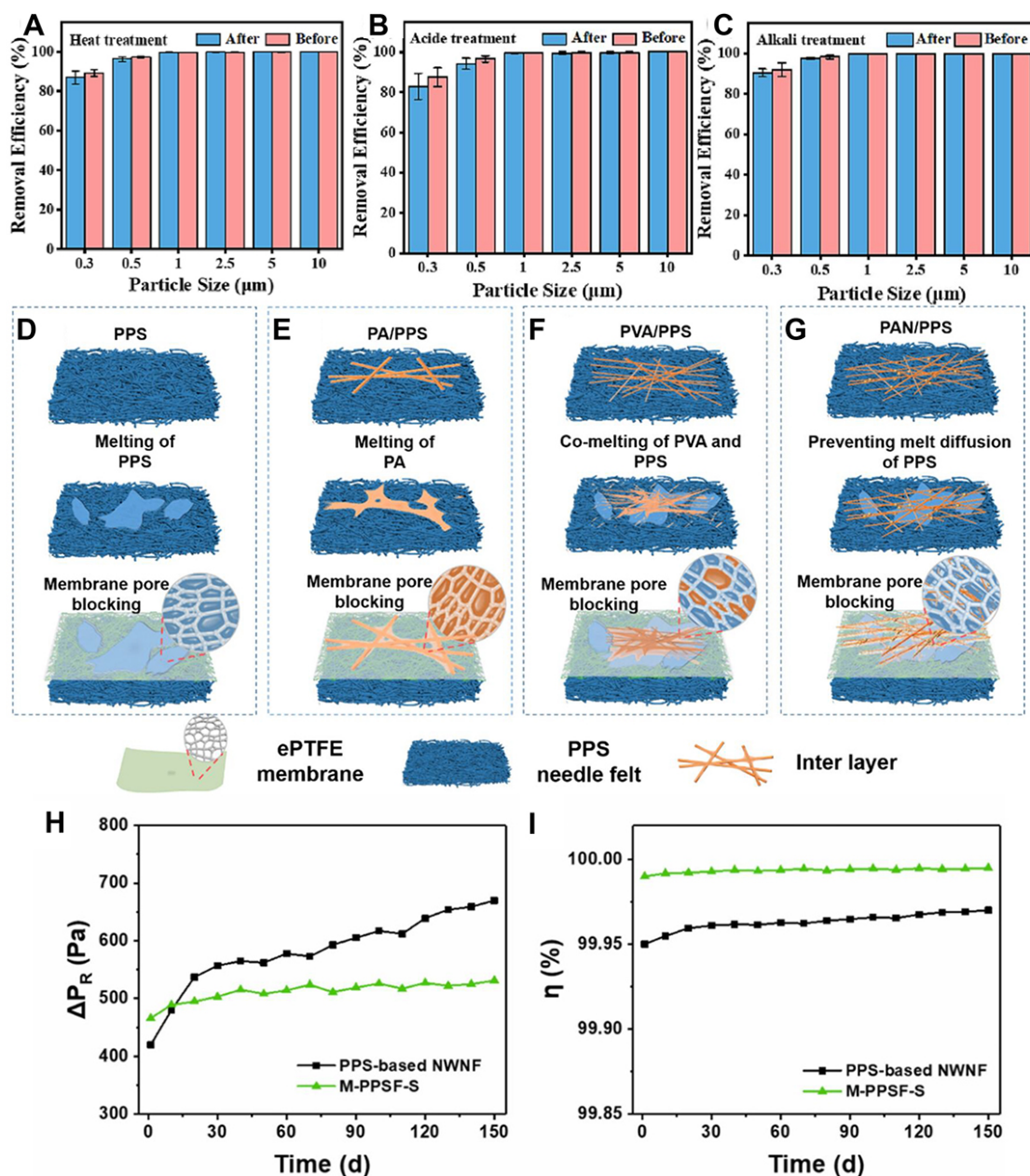


Figure 8. (A) PM_{2.5} filtration efficiency of the PPS/PPTA-70% ultrafine fiber felt before and after heat treatment at 230 °C for 48 h. (B) PM_{2.5} filtration efficiency of the PPS/PPTA-70% ultrafine fiber felt before and after acid treatment^[101]. (C) PM_{2.5} filtration efficiency of the PPS/PPTA-70% ultrafine fiber felt before and after alkali treatment^[101]. Schematic diagram of the composite mechanism of the (D) original ePTFE/PPS; (E) ePTFE/PA/PPS; (F) ePTFE/PVA/PPS; and (G) ePTFE/PAN/PPS composite filter. Comparisons of residual pressure drop ΔP_R ^[102] (H) and dedusting rate η (I) between PPS-based NWNFs and M-PPSF-Ss in the field test^[103].

fibrous membranes, which, in turn, increased the catalyst loading on the surface of the fibrous membranes. This synergistic growth effect of Fe and Mn also enhances the bonding strength between the catalyst and the fiber membrane, resulting in a high catalytic filtration efficiency of this PTFE/PPS fiber filtration membrane loaded with Mn_4FeO_x catalyst even under prolonged use. By modifying porous materials on the surface of membrane materials, it is possible to endow membrane materials with excellent properties such as photothermal conversion and gas adsorption^[106]. Metal-organic frameworks (MOFs) are novel porous crystalline materials with large specific surface area and nanocage structure. Zeolitic imidazolate

framework-8 (ZIF-8) is one of the stable and easy-to-prepare MOF materials^[107,108]. Yu *et al.* synthesized ZIF-8 for the adsorption of iodine vapors on the surface of melt-blown PPS fiber membranes by hydrothermal and biomimetic mineralization approaches^[39]. The mechanism of iodine vapor capture by PPS-ZIF-8-BSA (BSA, bovine serum albumin) membranes made by the biomimetic mineralization approach is shown in [Figure 9A](#). First, the nanocage structure and surface sites of ZIF-8 capture iodine molecules. Second, PPS phenyl captures iodine molecules through the π -I bonding. Finally, the nanoscale ZIF-8 and ultrafine PPS fiber membrane provided a large specific surface area for iodine capture. The PPS-ZIF-8 membrane gradually changes from yellow to black during the adsorption of iodine vapor [[Figure 9B](#)]. The maximum iodine adsorption capacity of PPS-ZIF-8 fiber membranes obtained by those two synthesis methods reached 2.51 and 2.07 g g⁻¹, respectively [[Figure 9C](#)]. Wang *et al.* constructed a ZIF-8@PPS fiber membrane with a layered lotus leaf papillary structure by growing ZIF-8 on the surface of nitric acid-treated melt-blown PPS fibers^[109]. Polar sulfur heteroatoms in the PPS structure induce electrostatic interactions between the fiber surface and ZIF-8, which, together with an increase in the roughness of the nitrified fiber surface, results in a strong combination of ZIF-8 with the PPS fiber surface. This nitration strategy provides a reference for the large-scale production of ZIF-8@PPS fiber membranes. For different sizes of PM, the filtration capacity of ZIF-8@PPS fiber membranes far exceeds that of ordinary PPS fiber membranes [[Figure 9D](#)]. ZIF-8@PPS fiber membranes still have good filtration ability even after different temperatures [[Figure 9E](#)] and different PH environments [[Figure 9F](#)]. Even with long-term cycling in this harsh environment, they still have good stability [[Figure 9G](#)].

PPS fiber filtration membranes have unique cost and performance advantages in the field of high-temperature exhaust gas purification in factories. However, the current research on the problems of insufficient filtration efficiency and high-temperature oxidation of PPS fiber filter membranes is still limited to the laboratory scale. Therefore, the development of high-efficiency and long-life PPS fiber filtration membranes for large-scale production and application is an urgent problem.

Chemical catalyst substrates

Improving the activity of a chemical catalytic reaction involves increasing the specific surface area of the catalyst. A larger specific surface area means that there are more active sites available for reactant molecules to interact with, which, in turn, increases the overall reaction rate. However, in industrial settings, chemical catalysts are often loaded onto a carrier material. Traditional carrier materials, such as metals with high electrical conductivity, are often inflexible and possess small specific surface area, making them unsuitable for certain applications. As a result, flexible carrier materials with large specific surfaces are considered the ideal choice for chemical catalysts. These materials provide a more efficient means of utilizing chemical catalysts, leading to improved performance and efficiency in various industrial processes^[110]. The high specific surface area and porosity of fiber membranes render them excellent flexible substrates for nanomaterials. By incorporating nanomaterials onto the surface of fiber membranes, not only can the adsorption, catalytic, and degradation properties of these nanomaterials be effectively harnessed, but also their practicality and reusability can be enhanced. Microfiber membranes possess submicron or even nanoscale surface areas, which offer substantial capacity for nanomaterial loading, thereby significantly boosting their catalytic potential^[111]. PPS fibers boast remarkable corrosion resistance, thermal stability, and dimensional stability, enabling them to endure harsh conditions without undergoing changes in their physical or chemical attributes^[70]. This makes PPS fiber membranes an ideal substrate for catalytic reactions with nanomaterials, especially in harsh environments. Remarkably, the ultra-fine PPS fiber membrane obtained through melt-blown spinning and melt electrostatic spinning can further amplify nanomaterial loading onto the surface of fibers, thereby bolstering its catalytic capabilities under rigorous conditions.

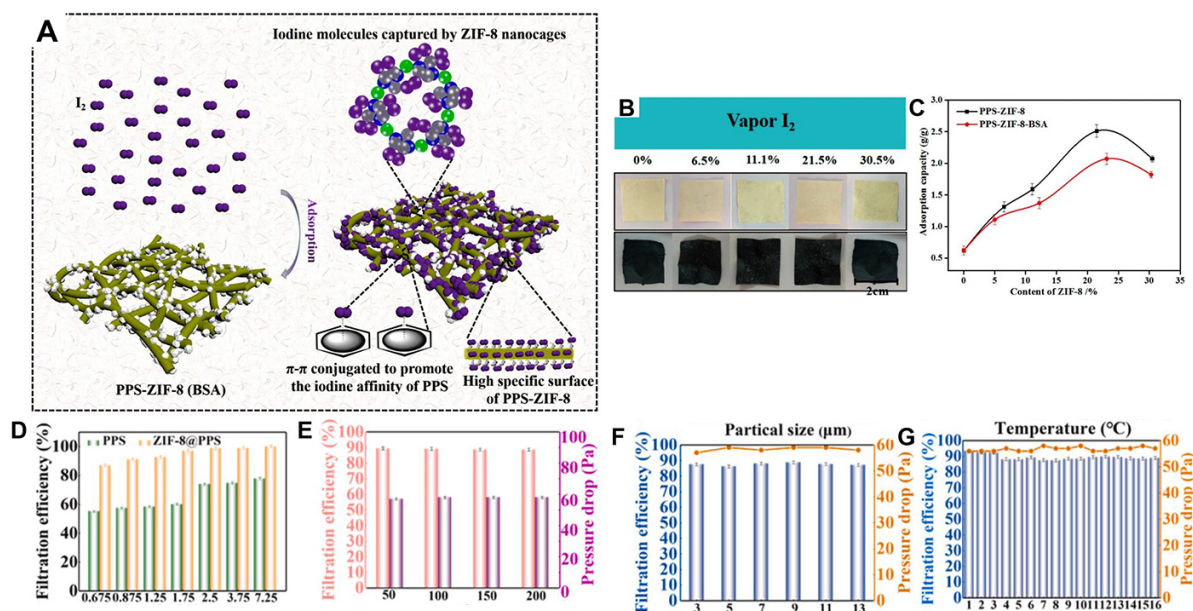


Figure 9. (A) Process of iodine vapor capture by the PPS-ZIF-8 (BSA) membrane. (B) Digital photos of the PPS-ZIF-8 membranes containing different ZIF-8 contents before and after iodine absorption. (C) Iodine adsorption capacities of PPS-ZIF-8 and PPS-ZIF-8-BSA containing different contents of ZIF-8^[39]. (D) Filtration efficiency of the ZIF-8@PPS and PPS membrane for DEHS airborne particles with various sizes. (E) Filtration capability of ZIF-8@PPS fibrous membrane that filtrates PM at different temperatures for 24 h. (F) Filtration capability of ZIF-8@PPS fibrous membrane to PM after different pH treatments for 24 h. (G) Long-term cycling stability of the ZIF-8@PPS fibrous membrane filtrating PM^[109].

PPS fibers have a smooth surface, which poses challenges for nanoparticles to adhere directly. As a remedy, sulfonation is frequently employed to establish a bond between the PPS fiber surface and the nanoparticle interface. This enables stable immobilization of nanoparticles onto the fiber membrane surface. Wang *et al.* utilized a precipitation method to load silver phosphate onto the surface of sulfonated PPS (SPPS) melt-blown fiber membranes^[112]. The high specific surface area of the melt-blown PPS fiber membrane provides ample sites for the growth of silver phosphate, significantly enhancing the photocatalytic activity of the $\text{Ag}_3\text{PO}_4/\text{SPPS}$ composite fiber membrane. Results revealed that with disodium hydrogen phosphate and silver nitrate concentrations of 0.06 and 0.3 mol, respectively, the composite fiber membrane displayed a degradation efficiency of 97.8% for a methylene blue (MB) solution within 30 min. The Fenton reaction, an inorganic chemical process, employs the Fenton reagent (a mixture of H_2O_2 and Fe^{2+}) to oxidize organic compounds to an inorganic state^[113]. The Fenton reactions are widely utilized for degrading organic pollutants in wastewater, involving significant consumption of hydrogen peroxide and ferrous ions^[114,115]. A pioneering catalytic approach involves decorating the Fenton catalyst onto the surfaces of a fiber membrane. This not only heightens catalytic efficiency but also enables Fenton catalyst reuse. Liu *et al.* developed a flexible PPS cathode membrane with aeration capability by filling a PPS melt-blown fiber membrane with conductive carbon black (CB)^[116]. The high porosity, effective adsorption, and numerous active sites in the PPS cathode membrane led to notably increased hydrogen peroxide production when employed in the electro-Fenton (e-Fenton) system [Figure 10A and B]. Efficient catalysis of most organic pollutants can be achieved in a maximum of 10 min under an e-Fenton catalytic system using a PPS cathode membrane [Figure 10C]. In addition, Liu further illustrated the realistic potential of PPS cathode membrane electrocatalytic elimination of pollutants by mineralization using TOC (total organic carbon) analysis [Figure 10D]. Hu *et al.* prepared PPS fiber membranes modified with ferrous oxalate (FeC_2O_4) for non-homogeneous Fenton processes by a chemical precipitation method^[117]. The SPPS fiber membrane effectively immobilized FeC_2O_4 particles on its surface, enhancing the operability and reusability of the

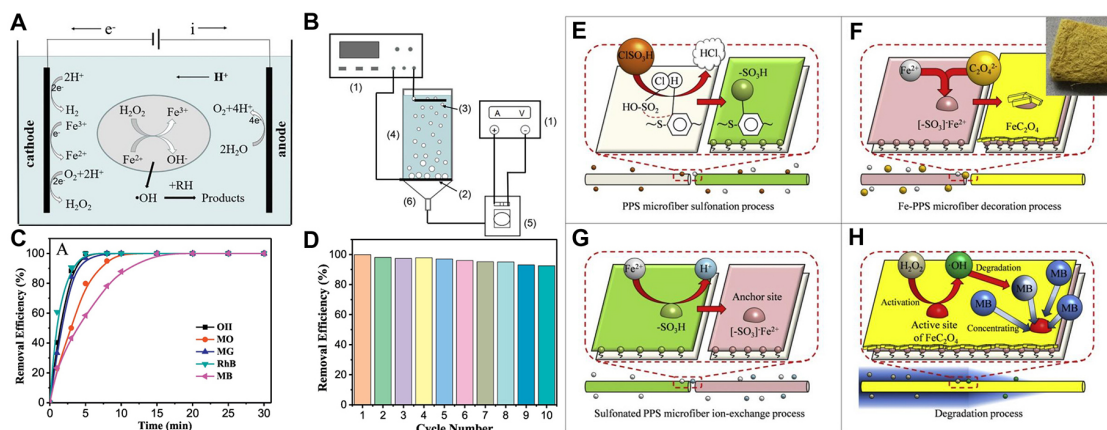


Figure 10. (A) Reaction mechanism of the e-Fenton process. (B) Schematic membrane of the electrolytic reactor, showing the (1) power supply, (2) PPS cathode film, (3) Pt foil, (4) reactor, (5) pumps, and (6) connecting device. Possible underlying mechanism of synthetic process and performance improvement. (C) Removal efficiency of contaminants. (D) The TOC (total organic carbon) removal efficiency of contaminants^[116]. (E) PPS microfiber sulfonation process; (F) sulfonated PPS microfiber ion-exchange process; (G) Fe-PPS microfiber decoration process; and (H) degradation process^[117].

composite fiber membrane catalyst. This catalyst facilitated OH^\bullet activation for efficient degradation of MB solutions, achieving a 99% degradation efficiency within 15 min. The PPS/ FeC_2O_4 composite fiber membrane catalyst could be reused after simple separation. The mechanism of the whole process can probably be explained as follows. Firstly, ClSO_3H attacks the benzene ring of PPS, causing it to carry a sulfonic acid group on the benzene ring [Figure 10E]. Then, Fe^{2+} exchanges H^+ on $-\text{SO}_2-\text{OH}$ in ferrous sulfate solution to form $[-\text{SO}_3]^- \text{Fe}^{2+}$ anchor localization sites on the fiber surface [Figure 10F]. When $\text{K}_2\text{C}_2\text{O}_4$ solution was added, the ferrous oxalate complex was immediately formed, thus allowing the fibers with anchoring sites to concentrate the complex. In addition, the SPPS layer was transformed into an interfacial layer, which strengthened the binding of the FeC_2O_4 catalyst to the PPS fibers [Figure 10G]. When the PPS/ FeC_2O_4 membrane is used for the Fenton reaction, OH^\bullet can be activated at the surface-active sites of PPS/ FeC_2O_4 [Figure 10H]. Thus, the catalytic degradation of organic molecules is realized.

PPS fiber membranes serve as excellent substrates for nanomaterials in catalysis applications. However, the smooth surfaces of PPS fibers often necessitate sulfonation before nanomaterial loading, which can compromise physical and chemical properties of fibers. Additionally, finer fiber membranes correspond to larger specific surface areas, implying greater nanoparticle loading potential. Thus, achieving finer PPS fiber membranes emerges as a pivotal strategy for enhancing catalytic capabilities.

Oil/water separation

The treatment of oily wastewater remains a pressing environmental concern^[118]. Traditional oil-water separation methods, such as centrifugation and flocculation, face issues of inefficiency, high costs, and secondary pollution^[119]. Sustainable membrane separation technology offers a viable solution to address this issue^[120]. However, conventional membrane materials often struggle to function effectively in harsh conditions, such as strong acids and alkaline^[121]. PPS fibers, with their exceptional corrosion resistance, emerge as an ideal choice for membrane materials in such challenging environments. Oil-water separation membranes generally fall into two categories: hydrophilic oleophobic membranes and hydrophobic oleophilic membranes. PPS fibers are hydrophobic and oleophilic. Consequently, research regarding the application of PPS fiber membranes in oil-water separation predominantly falls into two realms. One is to modify the surface of PPS fiber membranes to attain hydrophilic and oleophobic properties. The other is to enhance the hydrophobicity of PPS for the creation of superhydrophobic oleophilic PPS fiber membranes.

For instance, Huang *et al.* applied PE wax (PEW) powder and PTFE onto melt-blown PPS fiber membranes to prepare hydrophobic and oleophilic PPS fiber membranes^[122]. Similarly, Huang *et al.* employed the impregnation method to attach chitosan (CTS) onto melt-blown PPS fiber membranes, preparing hydrophilic and oleophobic PPS fiber membranes^[123]. These distinct PPS fiber membranes demonstrated selective permeability for either oil or water, underscoring their varying surface properties. Moreover, the high porosity of PPS fibers contributes to substantial flux during oil-water separation. Specifically, the flux of the two PPS fiber membranes for oil-water separation reached 3,500 and 2,250 L m⁻² h⁻¹, respectively. However, these techniques might not be optimally suited for large-scale oil-water separation applications. In a different approach, Fan *et al.* deposited graphene oxide (GO) on the melt-blown surface of a PPS fiber membrane and then converted graphene to reduced GO (rGO) using hydriodic acid^[124]. The process is detailed in Figure 11A. The resulting rGO@PPS composite fiber membrane not only displayed enhanced hydrophobicity and lipophilicity [Figure 11B-E] but also exhibited swift crude oil adsorption under Joule heating and solar heating, utilizing excellent conductivity and photothermal properties of rGO [Figure 11F]. The experimental outcomes indicated a reduction of 98.6% in crude oil adsorption time under Joule heating and a reduction of 97.3% under solar heating. Even though the high loading of rGO leads to a decrease in the flux of a rGO@PPS membrane, it still has a high flux [Figure 11G]. Meanwhile, the rGO@PPS membrane still has high separation efficiency after repeated cleaning [Figure 11H]. However, the immaturity of the melt-blown PPS fiber membrane process presents challenges for its large-scale application. Addressing this, Gao *et al.* employed a thermally induced phase separation (TIPS) method, combining PPS resins with papermaking PPS fiber membranes to craft a superhydrophobic PPS fiber membrane characterized by a rough concave structure and nanofiber network arrangement^[125]. Utilizing the same polymer materials mitigates performance degradation stemming from interfacial stability disparities. The distinctive concave features and nanofiber network significantly bolster the water-blocking capacity of the PPS fiber membrane. Notably, the superior porosity of the papermaking PPS fiber membrane, compared to its melt-blown counterpart, led to a higher oil-water separation flux of 7,350 L m⁻² h⁻¹.

Due to the industrial need for high-volume oil-water separation, research on PPS fiber membranes in this domain should prioritize scale-up applications. The papermaking PPS fiber membrane exhibits more promise for larger-scale use when compared to the melt-blown PPS fiber membrane. Additionally, the longevity of modified PPS fiber membranes should be considered, as certain modifications may inadvertently impair the integrity of PPS fibers. This aspect is vital in assessing the cost-effectiveness of PPS fiber membranes in the realm of oil-water separation.

CONCLUSION AND PERSPECTIVES

PPS fibers have been found to be highly suitable for use in challenging environments such as high temperatures, strong acids, and alkalis. Their exceptional corrosion resistance, thermal stability, and flame retardancy make PPS fiber membranes an ideal material for energy and environmental applications. In this paper, four types of preparation methods for PPS fiber membranes are discussed in detail: melt-blown spinning, melt electrostatic spinning, wet papermaking, and weaving. The PPS fiber membranes prepared through these four methods have discovered applications in diverse arenas, including lithium-ion batteries, AEL, chemical catalyst substrates, adsorption, and oil-water separation.

While ongoing research has made substantial advancements in PPS fiber membranes, prevalent issues across various preparation methods persist. High thickness, limited selectivity and permeability, and abbreviated service life collectively curtail the production and practical use of PPS fiber membranes. Difficulties in the preparation process are the main reason for limiting the development of PPS fiber membranes. Thus, the aspiration of achieving large-scale, high-performance PPS fiber membrane

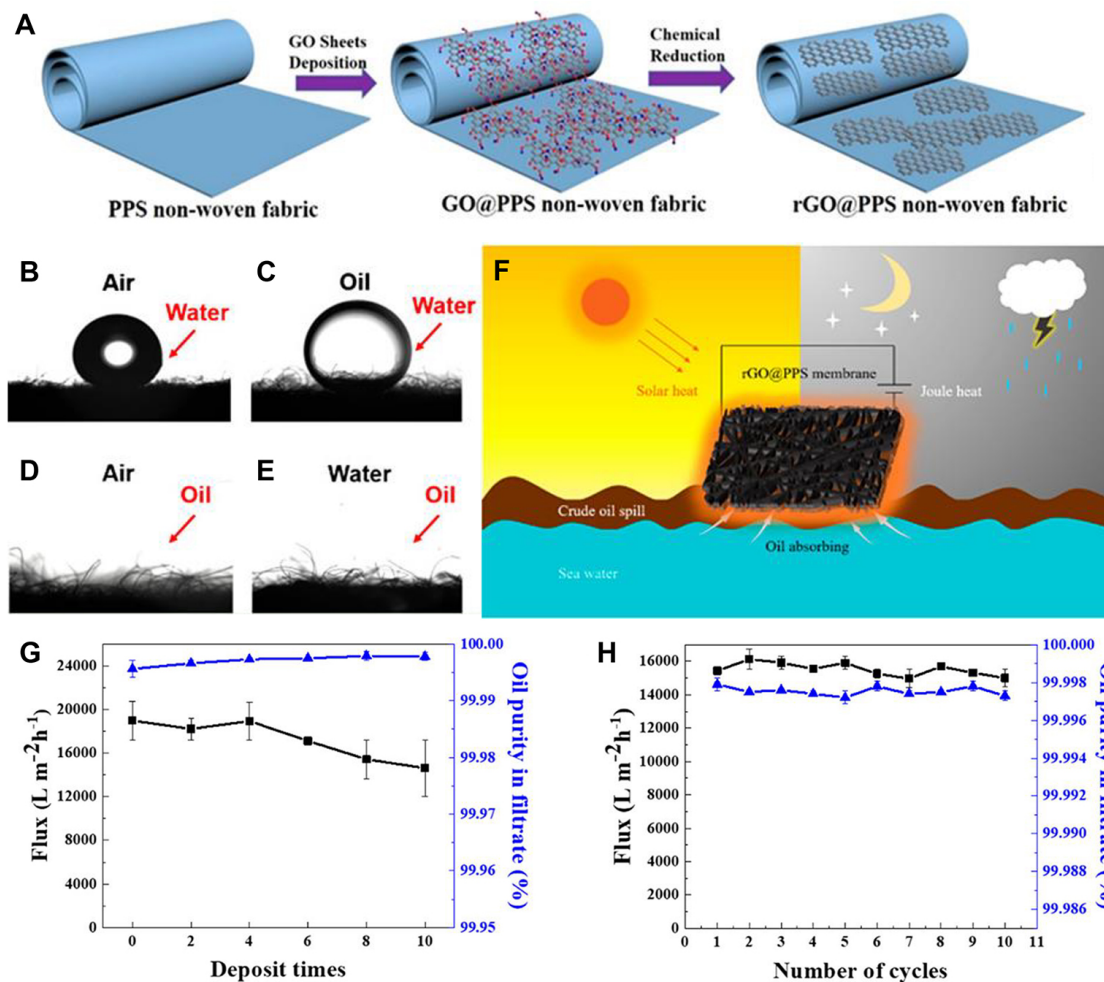


Figure 11. (A) Large-scale fabrication of rGO@PPS fibrous membrane. (B) Water contact angle in the air. (C) water contact angle under n-hexane. (D) Dichloromethane contact angle in the air. (E) Dichloromethane contact angle under water of M-8. (F) Reduction of crude oil adsorption time of PPS fiber membrane by Joule heat and solar heating. (G) Filtration flux and separation efficiency of rGO@PPS membrane with different deposition times. (H) Analysis of cycle performance of M-8 on kerosene/water mixture^[124].

production remains a formidable challenge. Forthcoming strides in research and development ought to focus on several pivotal dimensions to augment the performance and industrial viability of PPS fiber membranes:

(1) The realization of ultra-fine PPS membranes characterized by small fiber diameters is of great importance. A reduced fiber diameter precipitates heightened porosity and augmented specific surface area, concomitantly reducing the thickness of PPS fiber membranes and enhancing their selectivity and permeability. The crux of attaining ultrafine PPS fiber membranes resides in refining the preparation process.

(2) Exploring cost-effective methodologies that facilitate large-scale production of PPS fiber membranes is imperative. Presently preparation methods, encompassing melt-blown spinning, melt electrostatic spinning, wet papermaking, and weaving, exhibit varied limitations. While the melt-blown spinning engenders membranes with uneven pores unsuitable for direct application, melt electrostatic spinning is encumbered by immaturity and cost inefficiency. Both wet papermaking and weaving have the potential to produce PPS

fiber membranes on a large scale. However, the strength of PPS fiber membranes prepared by wet papermaking is insufficient, and the pore size of PPS fiber membranes prepared by weaving is too large.

(3) Enhancing the competitive prowess of PPS fiber membranes in the energy and environmental field stands as a pivotal pursuit. Presently, PPS fiber membranes have a quandary—lagging behind at the top and overshooting at the bottom. This signifies that while the costs undercut those of high-end aramid fiber membranes, the performance of high-temperature stability and mechanical strength is yet to match up. Although performance of high-temperature stability, corrosion resistance, and flame retardant surpasses those of regular fiber membranes, the relative costs remain steep. Addressing this challenge calls for a thorough exploration of the connection between the production process and the intended application domain. This endeavor facilitates the establishment of a harmonious equilibrium between cost and performance, leading to the creation of a PPS fiber membrane that stands out in terms of competitiveness.

In general, the main reason for the predicament of PPS fiber membranes is the difficulty and immaturity of the spinning and fiber membrane preparation process. The difficulties and immaturity of the process result in the high cost of PPS fiber membranes in membrane separation fields. Therefore, future research on these membranes should mainly focus on the spinning and fiber membrane preparation process.

DECLARATIONS

Authors' contributions

Searched a large amount of literature, wrote the manuscript, and obtained copyright licenses for all cited images in the manuscript: Zhu Q

Provide the research direction and funding support: Xu G

Discussed the review, including language checking and polishing: Zhu M, Hu Z, Zhang T, Zhu X, Zhang J, Shan M

Availability of data and materials

Not applicable.

Financial support and sponsorship

This work was financially supported by the National Key Research and Development Program of China (2022YFB3803502), National Natural Science Foundation of China (52103076), special fund of Beijing Key Laboratory of Indoor Air Quality Evaluate ion and Control (NO. BZ0344KF21-02), and State Key Laboratory of Electrical Insulation and Power Equipment (EIPE22203).

Conflicts of interest

All authors declared that there are no conflicts of interest.

Ethical approval and consent to participate

Not applicable.

Consent for publication

Not applicable.

Copyright

© The Author(s) 2024.

REFERENCES

1. de Mattos IL, de Castro MDL, Valcárcel M. Pervaporation: an integrated evaporation/gas-diffusion approach to analytical continuous separation techniques. *Talanta* 1995;42:755-63. DOI PubMed
2. Arosio P, Müller T, Mahadevan L, Knowles TPJ. Density-gradient-free microfluidic centrifugation for analytical and preparative separation of nanoparticles. *Nano Lett* 2014;14:2365-71. DOI PubMed
3. Zoccali M, Donato P, Mondello L. Recent advances in the coupling of carbon dioxide-based extraction and separation techniques. *Trends Analyt Chem* 2019;116:158-65. DOI
4. Zhang S, Ning S, Liu H, Wang X, Wei Y, Yin X. Preparation of ion-exchange resin via in-situ polymerization for highly selective separation and continuous removal of palladium from electroplating wastewater. *Sep Purif Technol* 2021;258:117670. DOI
5. Chen JP, Mou H, Wang LK, Matsuura T, Wei Y. Membrane separation: basics and applications. In: Wang LK, editor. Membrane and desalination technologies. Totowa, NJ: Humana Press; 2011. pp. 271-332. DOI
6. Strathmann H. Membrane separation processes: current relevance and future opportunities. *AIChE J* 2001;47:1077-87. DOI
7. Nazir A, Khan K, Maan A, Zia R, Giorno L, Schroën K. Membrane separation technology for the recovery of nutraceuticals from food industrial streams. *Trends Food Sci Technol* 2019;86:426-38. DOI
8. Liu HB, Li B, Guo LW, et al. Current and future use of membrane technology in the traditional Chinese medicine industry. *Sep Purif Rev* 2022;51:484-502. DOI
9. Ravanchi M, Kaghazchi T, Kargari A. Application of membrane separation processes in petrochemical industry: a review. *Desalination* 2009;235:199-244. DOI
10. Castel C, Favre E. Membrane separations and energy efficiency. *J Membr Sci* 2018;548:345-57. DOI
11. Goh SH, Lau HS, Yong WF. Metal-organic frameworks (MOFs)-based mixed matrix membranes (MMMs) for gas separation: a review on advanced materials in harsh environmental applications. *Small* 2022;18:e2107536. DOI PubMed
12. Visvanathan C, Aim RB, Parameshwaran K. Membrane separation bioreactors for wastewater treatment. *Crit Rev Environ Sci Technol* 2000;30:1-48. DOI
13. Li B, Qi B, Guo Z, Wang D, Jiao T. Recent developments in the application of membrane separation technology and its challenges in oil-water separation: a review. *Chemosphere* 2023;327:138528. DOI PubMed
14. Ulbricht M. Advanced functional polymer membranes. *Polymer* 2006;47:2217-62. DOI
15. Swolfs Y, Van den fonteyne W, Baets J, Verpoest I. Failure behaviour of self-reinforced polypropylene at and below room temperature. *Compos Part A Appl Sci Manuf* 2014;65:100-7. DOI
16. Zhang RC, Li R, Lu A, Jin Z, Liu B, Xu Z. The glass transition temperature of poly(phenylene sulfide) with various crystallinities. *Polym Int* 2013;62:449-53. DOI
17. Rahate AS, Nemade KR, Waghuley SA. Polyphenylene sulfide (PPS): state of the art and applications. *Rev Chem Eng* 2013;29:471-89. DOI
18. Hill Jr HW. History of polyphenylene sulfide. In: Seymour RB, Kirshenbaum GS, editors. High performance polymers: their origin and development. Dordrecht, The Netherlands: Springer; 1986. pp. 135-48. DOI
19. Cunningham BD, Huang J, Baird DG. Development of bipolar plates for fuel cells from graphite filled wet-lay material and a thermoplastic laminate skin layer. *J Power Sources* 2007;165:764-73. DOI
20. Gu J, Du J, Dang J, Geng W, Hu S, Zhang Q. Thermal conductivities, mechanical and thermal properties of graphite nanoplatelets/polyphenylene sulfide composites. *RSC Adv* 2014;4:22101-5. DOI
21. Wang XH, Qin YF, Wan JX, Li SB, Zhan Y, Ma YL. Research on the acid fastness of polyphenylene sulfide fiber. *Adv Mater Res* 2011;332-4:281-5. DOI
22. Guo Y, Bradshaw RD. Long-term creep of polyphenylene sulfide (PPS) subjected to complex thermal histories: the effects of nonisothermal physical aging. *Polymer* 2009;50:4048-55. DOI
23. Wang HC, Jiang DH, Liu Y. Life problem analysis on PPS filter application of bag dedusters in coal-fired power plants. *Adv Mater Res* 2011;236-8:2464-70. DOI
24. Lian D, Ren J, Han W, Ge C, Lu J. Kinetics and evolved gas analysis of the thermo-oxidative decomposition for neat PPS fiber and nano Ti-SiO₂ modified PPS fiber. *J Mol Struct* 2019;1196:734-46. DOI
25. Pan D, Lin P, Zhao L, et al. Polyphenylene sulfide scaffold based flexible supercapacitor electrode with competitive areal capacitance and flame-retardant behavior. *React Funct Polym* 2022;174:105216. DOI
26. Czerwiński W. Electronic processes in poly(p-phenylene) and related compounds, II. structure and electrical properties of polymers related to poly(p-phenylene sulfide). *Angew Makromol Chem* 1986;144:101-12. DOI
27. Lhymn C, Wapner P. Slurry erosion of polyphenylene sulfide-glass fiber composites. *Wear* 1987;119:1-11. DOI
28. Tan C, Yang Y, Gao J, Li S, Qing L. Temperature dependence of the elongation behavior of polyphenylene sulfide using melt spinning technique. *IOP Conf Ser Mater Sci Eng* 2017;274:012039. DOI
29. Song SS, White JL, Cakmak M. Structure development in the melt spinning and drawing of poly p phenylene sulfide fibers. *Int Polym Proc* 1989;4:96-102. DOI
30. Dandan L, Jianjun L, Lixin Y, Chao G, Baojun W. Effect of quercetin on the structure and oxidation resistance of polyphenylene sulfide fiber prepared by melt spinning. *Text Res J* 2023;93:3286-98. DOI
31. Xing J, Dai S, Chen Z, Wang Y, Zhang Z, Wang G. Effect of montmorillonite on the oxidative stability of polyphenylene sulfide

- fibers prepared by melt spinning. *Text Res J* 2022;92:2742-54. DOI
32. Carr PL, Ward IM. Drawing behaviour, mechanical properties and structure of poly(*p*-phenylene sulphide) fibres. *Polymer* 1987;28:2070-6. DOI
 33. Murthy NS, Elsenbaumer RL, Frommer JE, Baughman RH. Structural changes during annealing and during acceptor doping of oriented poly(*p*-phenylene sulfide). *Synth Met* 1984;9:91-6. DOI
 34. Zhang Y, Xiang PW, Zhang RP, Dai JM, Lian DD. Effect of spinning speed on structure and properties of poly-phenylene sulfide fiber. *Polym Mater Sci Eng* 2015;31:114-8. (In Chinese). DOI
 35. Gulgunje P, Bhat G, Spruiell J. Structure and properties development in poly(phenylene sulfide) fibers. II. effect of one-zone draw annealing. *J Appl Polym Sci* 2012;125:1890-900. DOI
 36. Hassounah IA, Rowland WC, Sparks SA, et al. Processing of multilayered filament composites by melt blown spinning. *J Appl Polym Sci* 2014;131:app.40786. DOI
 37. Xie S, Zeng YC. The effect of air pressure on the evolution of fiber path in melt-blowing process. *Adv Mater Res* 2014;852:496-500. DOI
 38. Hu JB, Liu F, Shao WL, Yue WL, Chen YK, Xiong JP. Research on melt-blown spinnability of PPS. *Shanghai Text Sci Technol* 2019;47:29-31. (in Chinese). DOI
 39. Yu Y, Ren L, Liu M, et al. Polyphenylene sulfide ultrafine fibrous membrane modified by nanoscale ZIF-8 for highly effective adsorption, interception, and recycling of iodine vapor. *ACS Appl Mater Interfaces* 2019;11:31291-301. DOI
 40. Zhou FL, Gong RH, Porat I. Mass production of nanofibre assemblies by electrostatic spinning. *Polym Int* 2009;58:331-42. DOI
 41. Jang SY, Seshadri V, Khil MS, et al. Welded electrochromic conductive polymer nanofibers by electrostatic spinning. *Adv Mater* 2005;17:2177-80. DOI
 42. Guo J, Wang T, Yan Z, Ji D, Li J, Pan H. Preparation and evaluation of dual drug-loaded nanofiber membranes based on coaxial electrostatic spinning technology. *Int J Pharm* 2022;629:122410. DOI PubMed
 43. Nayak R, Kyrtzis IL, Truong YB, et al. Fabrication and characterisation of nanofibres by meltblowing and melt electrospinning. *Adv Mater Res* 2012;472-5:1294-9. DOI
 44. Larrondo L, St John Manley R. Electrostatic fiber spinning from polymer melts. I. experimental observations on fiber formation and properties. *J Polym Sci Polym Phys Ed* 1981;19:909-20. DOI
 45. Li HY, Ding YM, Liu Y, Zhang YC, Yang WM. The preparation of polypropylene/polyvinyl alcohol ultra-fine fibers using melt electrospinning method. *Key Eng Mater* 2013;561:8-12. DOI
 46. An Y, Yu S, Li S, et al. Melt-electrospinning of polyphenylene sulfide. *Fibers Polym* 2018;19:2507-13. DOI
 47. Chen Q, Liu Y, Deng H, et al. Melt differential electrospinning of polyphenylene sulfide nanofibers for flue gas filtration. *Polym Eng Sci* 2020;60:2887-94. DOI
 48. Fan ZZ, He HW, Yan X, Zhao RH, Long YZ, Ning X. Fabrication of ultrafine PPS fibers with high strength and tenacity via melt electrospinning. *Polymers* 2019;11:530. DOI PubMed PMC
 49. Kou X, Han N, Zhang Y, et al. Fabrication of polyphenylene sulfide nanofibrous membrane via sacrificial templated-electrospinning for fast gravity-driven water-in-oil emulsion separation. *Sep Purif Technol* 2021;275:119124. DOI
 50. Balea A, Fuente E, Monte MC, et al. Industrial application of nanocelluloses in papermaking: a review of challenges, technical solutions, and market perspectives. *Molecules* 2020;25:526. DOI PubMed PMC
 51. Hui L, Yang B, Han X, Liu M. Application of synthetic fiber in air filter paper. *BioResources* 2018;13:4264-78. DOI
 52. Zhang M, Song S, Lu Z. Research and development status and related technology of synthetic fiber wet paper making. *China Paper* 2010;31:49-52. (in Chinese). Available from: <https://kns.cnki.net/KXReader/Detail?invoice=DapfgaPZrZN0oDNK0LXjqkPoOSw5AN4dtBTwH2B4QaAMFgi7E2GPimklbj3kgz0LWpFB3q%2BgCqIoAmk6WnYjAEWUmSdvJFEVjbzdJI5Q5X%2FKacI6WxcwE3VJBCMwHCnQVf%2FtBXglwcbLBGtXyz8yJRE4LgsdQ4YsvyubIZ8%3D&DBCODE=CJFQ&FileName=COKE201023017&TABLEName=cjfd2010&nonce=F495557B0C7F4EBBACFE33407A2C8C09&TIMESTAMP=1708481893825&uid=> [Last accessed on 1 Mar 2024]
 53. Zhu C, Zhang J, Xu J, et al. Facile fabrication of cellulose/polyphenylene sulfide composite separator for lithium-ion batteries. *Carbohydr Polym* 2020;248:116753. DOI
 54. Zhu C, Zhang J, Qiu S, Jia Y, Wang L, Wang H. Tailoring the pore size of polyphenylene sulfide nonwoven with bacterial cellulose (BC) for heat-resistant and high-wettability separator in lithium-ion battery. *Compos Commun* 2021;24:100659. DOI
 55. Zhu C, Zhang J, Xu J, et al. Aramid nanofibers/polyphenylene sulfide nonwoven composite separator fabricated through a facile papermaking method for lithium ion battery. *J Membr Sci* 2019;588:117169. DOI
 56. Yu Y, Jia G, Zhao L, et al. Flexible and heat-resistant polyphenylene sulfide ultrafine fiber hybrid separators for high-safety lithium-ion batteries. *Chem Eng J* 2023;452:139112. DOI
 57. Gong X, Chen X, Zhou Y. 4-advanced weaving technologies for high-performance fabrics. In: High-performance apparel materials, development, and applications Woodhead publishing series in textiles; 2018. pp.75-112. DOI
 58. Gandhi KL. 5 - the fundamentals of weaving technology. In: Woven textiles (second edition) principles, technologies and applications the textile institute book series; 2020. pp.167-270. DOI
 59. Mecha CA, Pillay VL. Development and evaluation of woven fabric microfiltration membranes impregnated with silver nanoparticles for potable water treatment. *J Membr Sci* 2014;458:149-56. DOI

60. Qiu C, Setiawan L, Wang R, Tang CY, Fane AG. High performance flat sheet forward osmosis membrane with an NF-like selective layer on a woven fabric embedded substrate. *Desalination* 2012;287:266-70. DOI
61. Lee HI, Mehdi M, Kim SK, et al. Advanced Zirfon-type porous separator for a high-rate alkaline electrolyser operating in a dynamic mode. *J Membr Sci* 2020;616:118541. DOI
62. Li M, Lu J, Chen Z, Amine K. 30 years of lithium-ion batteries. *Adv Mater* 2018;30:e1800561. DOI
63. Luiso S, Fedkiw P. Lithium-ion battery separators: recent developments and state of art. *Curr Opin Electrochem* 2020;20:99-107. DOI
64. Costa CM, Lee YH, Kim JH, Lee SY, Lancers-Méndez S. Recent advances on separator membranes for lithium-ion battery applications: from porous membranes to solid electrolytes. *Energy Stor Mater* 2019;22:346-75. DOI
65. Choi J, Kim PJ. A roadmap of battery separator development: past and future. *Curr Opin Electrochem* 2022;31:100858. DOI
66. Held M, Tuchschnid M, Zennegg M, et al. Thermal runaway and fire of electric vehicle lithium-ion battery and contamination of infrastructure facility. *Renew Sustain Energy Rev* 2022;165:112474. DOI
67. Klein S, Wrogemann JM, van Wickeren S, et al. Understanding the role of commercial separators and their reactivity toward LiPF_6 on the failure mechanism of high-voltage NCM523 || graphite lithium ion cells. *Adv Energy Mater* 2022;12:2102599. DOI
68. Jeong HS, Choi ES, Lee SY, Kim JH. Evaporation-induced, close-packed silica nanoparticle-embedded nonwoven composite separator membranes for high-voltage/high-rate lithium-ion batteries: advantageous effect of highly percolated, electrolyte-philic microporous architecture. *J Membr Sci* 2012;415-6:513-9. DOI
69. Luo D, Chen M, Xu J, et al. Polyphenylene sulfide nonwoven-based composite separator with superior heat-resistance and flame retardancy for high power lithium ion battery. *Compos Sci Technol* 2018;157:119-25. DOI
70. Zhang J, Zhu C, Xu J, et al. Enhanced mechanical behavior and electrochemical performance of composite separator by constructing crosslinked polymer electrolyte networks on polyphenylene sulfide nonwoven surface. *J Membr Sci* 2020;597:117622. DOI
71. Zeng X, Liu Y, He R, et al. Tissue paper-based composite separator using nano- SiO_2 hybrid crosslinked polymer electrolyte as coating layer for lithium ion battery with superior security and cycle stability. *Cellulose* 2022;29:3985-4000. DOI
72. Hu Y, Zhu G, Zeng X, et al. Tissue paper-based composite separator using double-crosslinked polymer electrolyte as coating layer for lithium-ion battery with superior ion transport and cyclic stability. *Cellulose* 2023;30:247-61. DOI
73. Zhang H, Liu J, Guan M, et al. Nanofibrillated cellulose (NFC) as a pore size mediator in the preparation of thermally resistant separators for lithium ion batteries. *ACS Sustain Chem Eng* 2018;6:4838-44. DOI
74. Trisno MLA, Dayan A, Lee SJ, et al. Reinforced gel-state polybenzimidazole hydrogen separators for alkaline water electrolysis. *Energy Environ Sci* 2022;15:4362-75. DOI
75. Guo Y, Li G, Zhou J, Liu Y. Comparison between hydrogen production by alkaline water electrolysis and hydrogen production by PEM electrolysis. *IOP Conf Ser Earth Environ Sci* 2019;371:042022. DOI
76. Renaud R, Leroy RL. Separator materials for use in alkaline water electrolyzers. *Int J Hydrog Energy* 1982;7:155-66. DOI
77. Modica G, Giuffrè L, Montoneri E, Pozzi V, Tempesti E. Electrolytic separators from asbestos cardboard: a flexible technique to obtain reinforced diaphragms or ion-selective membranes. *Int J Hydrog Energy* 1983;8:419-35. DOI
78. de Groot MT, Vreman AW. Ohmic resistance in zero gap alkaline electrolysis with a Zirfon diaphragm. *Electrochim Acta* 2021;369:137684. DOI
79. Zhu L, Song H, Zhang D, Wang G, Zeng Z, Xue Q. Negatively charged polysulfone membranes with hydrophilicity and antifouling properties based on in situ cross-linked polymerization. *J Colloid Interface Sci* 2017;498:136-43. DOI PubMed
80. Chung YT, Ng LY, Mohammad AW. Sulfonated-polysulfone membrane surface modification by employing methacrylic acid through UV-grafting: optimization through response surface methodology approach. *J Ind Eng Chem* 2014;20:1549-57. DOI
81. Teotia RS, Kalita D, Singh AK, Verma SK, Kadam SS, Bellare JR. Bifunctional polysulfone-chitosan composite hollow fiber membrane for bioartificial liver. *ACS Biomater Sci Eng* 2015;1:372-81. DOI PubMed
82. Aerts P, Kuypers S, Genné I, et al. Polysulfone-ZrO₂ surface interactions. The influence on formation, morphology and properties of zirfon-membranes. *J Phys Chem B* 2006;110:7425-30. DOI
83. Xu L, Li W, You Y, Zhang S, Zhao Y. Polysulfone and zirconia composite separators for alkaline water electrolysis. *Front Chem Sci Eng* 2013;7:154-61. DOI
84. Oh SJ, Kim N, Lee YT. Preparation and characterization of PVDF/TiO₂ organic-inorganic composite membranes for fouling resistance improvement. *J Membr Sci* 2009;345:13-20. DOI
85. Lee JW, Lee C, Lee JH, et al. Cerium oxide-polysulfone composite separator for an advanced alkaline electrolyzer. *Polymers* 2020;12:2821. DOI PubMed PMC
86. Sun YP. Post-processing effect on the performance of PPS fiber membrane for water electrolyzer hydrogen production. *J Ind Text* 2015;33:14-7. Available from: https://kns.cnki.net/kcms2/article/abstract?v=Y2wviAwYInKCFOnL-zI2KtFSP29ofZH8v1rUhfOUoTRi44jfw2T4q8M288fEprRS69p1R14Z9hfGXiN_XoPbO79terPbaDM0Vh0yetySeSnGOqk1IV4xoOLh8JluZYQQyYpCCxIssyA=&uniplatform=NZKPT&language=CHS [Last accessed on 1 Mar 2024]
87. Su YP. The preparation and performance of polyphenylene sulfide staple fibers and filament diaphragm. *J Henan Univ Eng* 2022;34:04. DOI
88. Liang CZ, Chung TS, Lai JY. A review of polymeric composite membranes for gas separation and energy production. *Prog Polym Sci* 2019;97:101141. DOI

89. Vermeiren PH, Leysen R, Beckers H, Moreels JP, Claes A. The influence of manufacturing parameters on the properties of macroporous Zirfon® separators. *J Porous Mater* 2008;15:259-64. DOI
90. Schalenbach M, Lueke W, Stolten D. Hydrogen diffusivity and electrolyte permeability of the Zirfon PERL separator for alkaline water electrolysis. *J Electrochem Soc* 2016;163:F1480-8. DOI
91. In Lee H, Dung DT, Kim J, et al. The synthesis of a Zirfon-type porous separator with reduced gas crossover for alkaline electrolyzer. *Int J Energy Res* 2020;44:1875-85. DOI
92. Ali MF, Lee HI, Bernäcker CI, et al. Zirconia toughened alumina-based separator membrane for advanced alkaline water electrolyzer. *Polymers* 2022;14:1173. DOI PubMed PMC
93. Lee JW, Lee JH, Lee C, et al. Cellulose nanocrystals-blended zirconia/polysulfone composite separator for alkaline electrolyzer at low electrolyte contents. *Chem Eng J* 2022;428:131149. DOI
94. Francis CFJ, Kyrazis IL, Best AS. Lithium-ion battery separators for ionic-liquid electrolytes: a review. *Adv Mater* 2020;32:e1904205. DOI PubMed
95. Manabe A, Domon H, Kosaka J, Hashimoto T, Okajima T, Ohsaka T. Study on separator for alkaline water electrolysis. *J Electrochem Soc* 2016;163:F3139-45. DOI
96. Jbaily A, Zhou X, Liu J, et al. Air pollution exposure disparities across US population and income groups. *Nature* 2022;601:228-33. DOI PubMed PMC
97. Clappier A, Thunis P, Beekmann M, Putaud JP, de Meij A. Impact of SO_x, NO_x and NH₃ emission reductions on PM_{2.5} concentrations across Europe: hints for future measure development. *Environ Int* 2021;156:106699. DOI PubMed PMC
98. Tanthapanichakoon W, Hata M, Nitta KH, Furuuchi M, Otani Y. Mechanical degradation of filter polymer materials: polyphenylene sulfide. *Polym Degrad Stab* 2006;91:2614-21. DOI
99. Tanthapanichakoon W, Furuuchi M, Nitta KH, Hata M, Endoh S, Otani Y. Degradation of semi-crystalline PPS bag-filter materials by NO and O₂ at high temperature. *Polym Degrad Stab* 2006;91:1637-44. DOI
100. Tanthapanichakoon W, Furuuchi M, Nitta KH, Hata M, Otani Y. Degradation of bag-filter non-woven fabrics by nitric oxide at high temperatures. *Adv Powder Technol* 2007;18:349-54. DOI
101. Zhao P, Yan J, Chen C, et al. PPS ultrafine fiber enhanced aramid fiber filter with superior thermal stability and excellent chemical resistance for efficient PM_{2.5} removal. *React Funct Polym* 2023;188:105605. DOI
102. Ye W, Feng S, Zhou Q, Zhang F, Zhong Z, Xing W. Gridded fibers' restricted melting strategy for gas permeance and binding enhancement of the ePTFE/PPS filter. *Ind Eng Chem Res* 2023;62:9503-14. DOI
103. Zhang B, Wang W, Cao H, et al. Development of an asymmetric composite PPS-based bag-filter material through membrane laminating and superfine fiber blending: lab test, field application and development of numerical models. *J Hazard Mater* 2023;459:132078. DOI
104. Zheng WJ, Zheng YY, Chen J, Zou HQ, Fu BB, Chen XH. Fabrication of nf-MnO₂/PPS functional composites for selective reduction of NO_x with NH₃. *Acta Polym Sinica* 2017;11:1806-15. DOI
105. Luo R, Zeng Y, Ju S, et al. Flowerlike FeO_x-MnO_x amorphous oxides anchored on PTFE/PPS membrane for efficient dust filtration and low-temperature no reduction. *Ind Eng Chem Res* 2022;61:5816-24. DOI
106. Li H, Hu C, He Y, Sun Z, Yin Z, Tang D. Emerging surface strategies for porous materials-based phase change composites. *Matter* 2022;5:3225-59. DOI
107. DeCoste JB, Peterson GW. Metal-organic frameworks for air purification of toxic chemicals. *Chem Rev* 2014;114:5695-727. DOI PubMed
108. Bux H, Feldhoff A, Cravillon J, Wiebcke M, Li Y, Caro J. Oriented zeolitic imidazolate framework-8 membrane with sharp H₂/C₃H₈ molecular sieve separation. *Chem Mater* 2011;23:2262-9. DOI
109. Wang W, Hou Z, Zhang H, et al. Harsh environmental-tolerant ZIF-8@polyphenylene sulfide membrane for efficient oil/water separation and air filtration under extreme conditions. *J Membr Sci* 2023;685:121885. DOI
110. Vankelecom IFJ. Polymeric membranes in catalytic reactors. *Chem Rev* 2002;102:3779-810. DOI PubMed
111. Liu JW, Liang HW, Yu SH. Macroscopic-scale assembled nanowire thin films and their functionalities. *Chem Rev* 2012;112:4770-99. DOI PubMed
112. Wang P, He C, Hu L, et al. Load of Ag₃PO₄ particles on sulfonated polyphenylene sulfide superfine fibre with high visible-light photocatalytic activity. *Fibers Polym* 2018;19:1379-85. DOI
113. Huston PL, Pignatello JJ. Degradation of selected pesticide active ingredients and commercial formulations in water by the photo-assisted Fenton reaction. *Water Res* 1999;33:1238-46. DOI
114. Azbar N, Yonar T, Kestioglu K. Comparison of various advanced oxidation processes and chemical treatment methods for COD and color removal from a polyester and acetate fiber dyeing effluent. *Chemosphere* 2004;55:35-43. DOI PubMed
115. Chen W, Yang X, Huang J, et al. Iron oxide containing graphene/carbon nanotube based carbon aerogel as an efficient E-Fenton cathode for the degradation of methyl blue. *Electrochim Acta* 2016;200:75-83. DOI
116. Liu M, Yu Y, Xiong S, et al. A flexible and efficient electro-fenton cathode film with aeration function based on polyphenylene sulfide ultra-fine fiber. *React Funct Polym* 2019;139:42-9. DOI
117. Hu L, Liu Z, He C, et al. Ferrous-oxalate-decorated polyphenylene sulfide fenton catalytic microfiber for methylene blue degradation. *Compos Part B Eng* 2019;176:107220. DOI
118. Chu Z, Feng Y, Seeger S. Oil/water separation with selective superantwetting/superwetting surface materials. *Angew Chem Int Ed*

- 2015;54:2328-38. [DOI](#) [PubMed](#)
119. Zhang R, Xu Y, Shen L, Li R, Lin H. Preparation of nickel@polyvinyl alcohol (PVA) conductive membranes to couple a novel electrocoagulation-membrane separation system for efficient oil-water separation. *J Membr Sci* 2022;653:120541. [DOI](#)
 120. Adebajo MO, Frost RL, Kloprogge JT, Carmody O, Kokot S. Porous materials for oil spill cleanup: a review of synthesis and absorbing properties. *J Porous Mater* 2003;10:159-70. [DOI](#)
 121. Cao Y, Zhang X, Tao L, et al. Mussel-inspired chemistry and Michael addition reaction for efficient oil/water separation. *ACS Appl Mater Interfaces* 2013;5:4438-42. [DOI](#)
 122. Huang H, Liu M, Li Y, et al. Polyphenylene sulfide microfiber membrane with superhydrophobicity and superoleophilicity for oil/water separation. *J Mater Sci* 2018;53:13243-52. [DOI](#)
 123. Huang H, Li Y, Zhao L, et al. A facile fabrication of chitosan modified PPS-based microfiber membrane for effective antibacterial activity and oil-in-water emulsion separation. *Cellulose* 2019;26:2599-611. [DOI](#)
 124. Fan T, Su Y, Fan Q, et al. Robust graphene@PPS fibrous membrane for harsh environmental oil/water separation and all-weather cleanup of crude oil spill by joule heat and photothermal effect. *ACS Appl Mater Interfaces* 2021;13:19377-86. [DOI](#)
 125. Gao Y, Qi Y, Wang S, Zhou X, Lyu L, Jin G. Superhydrophobic polyphenylene sulfide fiber paper with nanofiber network-like structure prepared via regulation of TIPS process for oil/water separation. *J Mater Sci* 2022;57:20531-42. [DOI](#)